

THEORETICAL ANALYSIS OF CORROSION FOR CARBON STEEL UNDER TWO PHASE FLOW CONDITIONS

A Thesis

**Submitted to the College of Engineering
of Nahrain University in Partial Fulfillment
of the Requirements for the Degree of
Master of Science
in
Chemical Engineering**

by

Mariam H. Fawzi

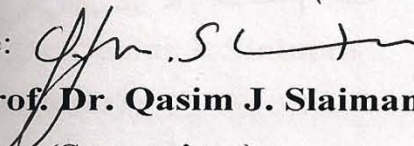
(B. Sc. In Chemical Engineering 2005)

**Muharram
January**

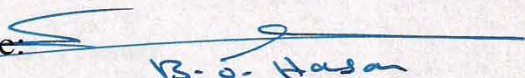
**1430
2009**

Certification

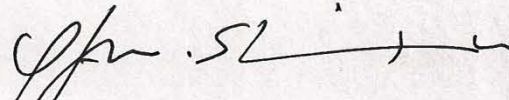
We certify that this thesis entitled **"Theoretical Analysis of Corrosion For Carbon Steel Under Two Phase Flow Conditions"** was prepared by **Mariam H. Fawzi** under our supervision at Nahrain University/College of Engineering in partial fulfillment of the requirements for the degree of Master of Science in Chemical Engineering.

Signature: 
Name: **Prof. Dr. Qasim J. Slaiman**
(Supervisor)

Date: / /

Signature: 
Name: **Dr. Basim O. Hasan**
(Supervisor)

Date: 28 / 2 / 2009

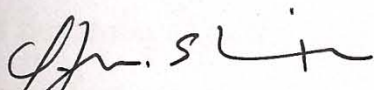
Signature: 
Name: **Prof. Dr. Qasim J. Slaiman**
(Head of Department)

Date: / /

Certificate

We certify, as an examining committee, that we have read this thesis entitled **"Theoretical Analysis of Corrosion For Carbon Steel Under Two Phase Flow Conditions"**, examined the student **Mariam H. Fawzi** in its content and found it meets the standard of thesis for the degree of Master of Science in Chemical Engineering.

Signature:



Name: **Prof. Dr. Qasim J. Slaiman**

(Supervisor)

Date:

/ /

Signature:



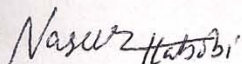
Name: **Dr. Basim O. Hasan**

(Supervisor)

Date:

25 / 2 / 2009

Signature:



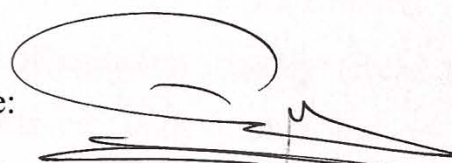
Name: **Dr. Naseer A. Habobi**

(Member)

Date:

10 / 3 / 2009

Signature:



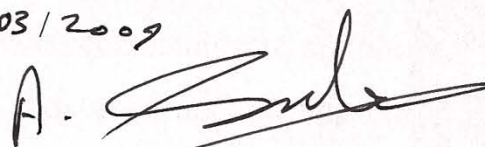
Name: **Ass. Prof. Dr. Mohammed H. Hafiz**

(Member)

Date:

01 / 03 / 2009

Signature:



Name: **Prof. Dr. Abbas H. Sulaymon**

(Chairman)

Date:

/ /

Approval of the College of Engineering

Signature:



Name: **Prof. Dr. Muhsin J. Jweeg**

(Dean)

Date:

8 / 4 / 2009

ABSTRACT

For continuation of the experimental data of Atwan and Aziz, a theoretical analysis was carried out to show the influence of two phase flow on corrosion under two different temperatures 25 and 40 °C. It is also aimed to understand the agitation of these two phase flow under different conditions at different agitation velocities.

They used two liquids. These are water and kerosene. Water was used at different percentages of the total volume. These percentages range from 1% to 30%. The effect of agitation and water percentage on corrosion were studied and recorded.

To evaluate the results, analysis of variance methods were used. This method indicates that at 25 °C the velocity of agitation impeller (Re) has a clear effect on corrosion, number of droplets per unit volume and on the diameter of these droplets.

It has been found that the water percentage affects corrosion rate and the diameter of droplets formed. On the other hand, it has been noticed that the water percentage has no effect on the number of droplets per unit volume. However, the effect of water percentage on corrosion rate found more than the effect of velocity of agitation. The same is true for the diameter of droplets formed.

The analysis of variance at 40 °C indicates that the velocity of agitation affects the corrosion rate, number of droplets per unit volume and the diameter of droplets formed.

The analysis of variance also indicates that the water percentage has more effect on corrosion rate while the velocity of agitation has more effect on the diameter of droplets formed.

These findings are obtained from experimental results adopted in this analysis. It has been also found that the higher the temperature, the lesser corrosion takes place. The reason could be attributed to the fact that the temperature reduces the oxygen in aqueous phase therefore, reduces the corrosion rate.

The placement of metal specimens in the agitation vessel is also important as found by the present analysis. The specimens close to the rotating impeller shaft are influenced differently from specimens placed at the wall of agitation vessel. This is because the intensity of turbulence and number of droplets per unit volume are not similar at different locations in the agitation vessel.

List of Contents

Abstract	I
List of Contents	III
Nomenclature	VI
List of Tables	VIII
List of Figures	X

Chapter One

INTRODUCTION

1-1	Introduction	1
1-2	Aim of project	4

Chapter Two

CORROSION

2.1	Corrosion under Two Phase Flow	6
2.2	Oxidation and reduction	10
2.3	Type of corrosion	11
2.3.1	Uniform corrosion	11
2.3.2	Galvanic corrosion	12
2.3.3	Pitting corrosion	13
2.3.4	Crevice corrosion	14
2.3.5	Erosion corrosion	15
2.4	Polarization	16
2.4.1	Activation polarization	16
2.4.2	Concentration polarization	18
2.4.3	Resistant polarization	20

2.4.4	Combined polarization	21
2.5	Electrochemical mechanism of corrosion rate	22
2.6	Factors affecting corrosion rate	23
2.7	Bubble flow	24
2.8	Characteristics of agitation	24
2.9	Agitation and mixing of liquids	25
2.9.1	Purpose of agitation	25
2.9.2	Agitated vessels	26
2.9.3	Impellers	27
2.9.4	Turbine	27
2.9.5	Slandered turbine design	28
2.10	Phase inversion of liquid- liquid dispersion in agitated vessel	30
2.11	Flow pattern in agitation	31
2.12	Mass transfer to suspension of small particles	32
2.13	Two ways analysis of variance	34

Chapter Three

RESULTS AND CALCULAIONS

3.1	Introduction	38
3.2	Reynold's number	38
3.3	Weber number	39
3.4	Sauter mean diameter	40
3.5	Number of droplets	40
3.6	Mass transfer coefficient	47

3.7	Two ways analysis (ANOVA)	54
-----	---------------------------	----

Chapter Four

DISCUSSION

4.1	Introduction	62
4.2	Single phase (100% Vol. aqueous solution)	62
4.3	Two phase (water/ oil)	63
4.3.1	Effects of Reynold numbers and Weber number	63
4.3.2	Oxygen concentration	80
4.3.3	Aqueous phase	82
4.3.4	Effect of droplets	83
4.3.5	Effect of flow pattern	89

Chapter Five

CONCLUSIONS AND RECOMMENDATIONS

5.1	Conclusions	92
5.2	Recommendations	92
	References	93

Appendix A

Appendix B

Appendix C

NUMACULATURE

C	=	Corrosion Factor.
c	=	Concentration of diffusion ion (mol/m ³).
D	=	Diffusion coefficient (m ² /s).
d	=	Diameter of metal (m).
D _a	=	Impeller diameter (m).
d ₃₂	=	Sauter mean diameter (m).
E	=	Potential.
F	=	Faraday number.
i	=	Rate of oxidation or reduction.
i _L	=	Limiting current density.
k	=	Mass transfer coefficient (m/s).
l	=	Length of metal (m).
n	=	Number of electrons.
N _I	=	Rotational speed of impeller (rpm).
p/v	=	Power input per unit volume (J/m ³).
R	=	Constant.
Re	=	Reynold number = $l u_b \rho / \mu$.
Sc	=	Schmidt number = $\mu / \rho D$.
Sh	=	Sherwood number = $k l / D$.
T	=	Temperature (C).
We	=	Weber number.

Greek Symbols

β	=	Tafel constant.
Ψ	=	Volumetric fraction gas or liquid hold up in dispersion.
μ	=	Fluid viscosity (poise).
δ	=	Thickness of stagnant layer.
ρ	=	Density of fluid (Kg/m ³).
η_a	=	Overvoltage.
γ	=	Constant.
λ	=	Constant.
α	=	Constant.

Abbreviations

MSC	=	Columns sum squares.
MSE	=	Error sum squares.
MSR	=	Row sum square.
M.wt	=	Molecular weight.
SSC	=	Columns sum of square.
SSI	=	Total sum of square
SST	=	Total sum of square

List of Tables

<u>Table No.</u>	<u>Title</u>	<u>Page</u>
Table (2-1)	Design equations of agitator (cylinder).	28
Table (3-1)	Total number of droplets at 25 C ⁰ .	42
Table (3-2)	Total number of droplets at 40 C ⁰ .	43
Table (3-3)	The number of drops striking the specimen/ second at 25 C ⁰	44
Table (3-4)	The number of drops striking the specimen/ second at 40 C ⁰	45
Table (3-5)	Mass transfer coefficient calculated from experimental corrosion rate of iron in a mixture of kerosene and water at 25 C ⁰ .	48
Table (3-6)	Mass transfer coefficient calculated from experimental corrosion rate of iron in a mixture of kerosene and water at 40 C ⁰ .	49
Table (3-7)	Mass transfer coefficient calculated from equation (4-12) at 25C ⁰ .	50
Table (3-8)	Mass transfer coefficient calculated from equation (4-12) at 40C ⁰ .	51
Table (3-9)	Corrosion rate calculated from equation (4-12) at 25C ⁰ .	51
Table (3-10)	Corrosion rate calculated from equation (4-12) at 40C ⁰ .	52
Table (3-11)	Data of C.R. at 25 ⁰ C.	54
Table (3-12)	Analysis of variance for C.R. at 25 ⁰ C .	56
Table (3-13)	Data of Sauter mean diameter at 25 ⁰ C.	57

Table (3-14)	Analysis of variance for Sauter mean diameter at 25 ⁰ C.	58
Table (3-15)	Data of total number of droplets per unit volume at 25 ⁰ C.	58
Table (3-16)	Analysis of variance for total number of droplets per unit volume at 25 ⁰ C.	59
Table (3-17)	Data of Corrosion rate at 40 ⁰ C.	59
Table (3-18)	Analysis of variance for Corrosion rate at 40 ⁰ C.	59
Table (3-19)	Data of Sauter mean diameter at 40 ⁰ C.	60
Table (3-20)	Analysis of variance for Sauter mean diameter at 40 ⁰ C.	60
Table (3-21)	Data of total number of droplets per unit volume at 40 ⁰ C.	61
Table (3-22)	Analysis of variance for total number of droplets per unit volume at 40 ⁰ C.	61
Table (4-1)	Summery of two way analysis at 25 ⁰ C	89
Table (4-2)	Summery of two way analysis at 40 ⁰ C	89

List of figures

<u>Figure No.</u>	<u>Title</u>	<u>Page</u>
Figure (2-1)	Hydrogen – reduction reaction under activation polarization	18
Figure (2-2)	Concentration polarization during hydrogen reduction	19
Figure (2.3)	Combined Polarization curve	21
Figure (2.4)	Typical agitation process vessel	26
Figure (2.5)	Types of turbine impellers	28
Figure (2.6)	Measurements of turbine	30
Figure(2.7)	Disk flat blade turbine (a) without baffles .(b) with baffles	32
Figure(2.8)	Power correlation for various impellers and baffles.	33
Figure (4-1)	Relation between corrosion rate (experimental and calculated) vs. Reynolds number at 40 °C , %water=0.01.	65
Figure (4-2)	Relation between corrosion rate (experimental and calculated) vs. Reynolds number at 40 °C , %water=0.05.	65
Figure (4-3)	Relation between corrosion rate (experimental and calculated) vs. Reynolds number at 40 °C , %water=0.1.	66
Figure (4-4)	Relation between corrosion rate (experimental and calculated) vs. Reynolds number at 40 °C , %water=0.2.	66

Figure (4-5)	Relation between corrosion rate (experimental and calculated) vs. Reynolds number at 25 °C , %water=0.05.	67
Figure (4-6)	Relation between corrosion rate (experimental and calculated) vs. Reynolds number at 25 °C , %water=0.15.	67
Figure (4-7)	Relation between corrosion rate (experimental and calculated) vs. Reynolds number at 25 °C , %water=0.3.	68
Figure (4-8)	Relation between Reynolds number and total number of droplets per unit volume at 25 °C , %water=0.05.	68
Figure (4-9)	Relation between log total number of droplets per unit volume and log Reynolds number at 25 °C , %water=0.05.	69
Figure (4-10)	Relation between Reynolds number and total number of droplets per unit volume at 25 °C, %water=0.15.	69
Figure (4-11)	Relation between log total number of droplets per unit volume and log Reynolds number at 25 °C, %water=0.15.	70
Figure (4-12)	Relation between Reynolds number and total number of droplets per unit volume at 25 °C, %water=0.3.	70
Figure (4-13)	Relation between log total number of droplets per unit volume and log Reynolds number at 25 °C,	

	%water=0.3.	71
Figure (4-14)	Relation between Reynolds number and total number of droplets per unit volume at 40 °C , %water=0.01.	71
Figure (4-15)	Relation between log total number of droplets per unit volume and log Reynolds number at 40 °C , %water=0.01.	72
Figure (4-16)	Relation between Reynolds number and total number of droplets per unit volume at 40 °C , %water=0.05.	72
Figure (4-17)	Relation between log total number of droplets per unit volume and log Reynolds number at 40 °C , %water=0.05.	73
Figure (4-18)	Relation between Reynolds number and total number of droplets per unit volume at 40 °C , %water=0.1.	73
Figure (4-19)	Relation between log total number of droplets per unit volume and log Reynolds number at 40 °C , %water=0.1.	74
Figure (4-20)	Relation between Reynolds number and total number of droplets per unit volume at 40 °C , %water=0.2.	74
Figure (4-21)	Relation between log total number of droplets per unit volume and log Reynolds number at 40 °C , %water=0.2.	75
Figure (4-22)	Relation between corrosion rate (experimental	

	and calculated) vs. Weber number at 40 °C , %water=0.01.	765
Figure (4-23)	Relation between corrosion rate (experimental and calculated) vs. Weber number at 40 °C , %water=0.05.	76
Figure (4-24)	Relation between corrosion rate (experimental and calculated) vs. Weber number at 40 °C, %water=0.1.	76
Figure (4-25)	Relation between corrosion rate (experimental and calculated) vs. Weber number at 40 °C, %water=0.2.	77
Figure (4-26)	Relation between corrosion rate (experimental and calculated) vs. Weber number at 25 °C, %water=0.05.	77
Figure (4-27)	Relation between corrosion rate (experimental and calculated) vs. Weber number at 25 °C, %water=0.15.	78
Figure (4-28)	Relation between corrosion rate (experimental and calculated) vs. Weber number at 25 °C, %water=0.3.	78
Figure (4-29)	Relation between corrosion rate (experimental and calculated) vs. number of droplets at 40 °C, %water=0.01.	84
Figure (4-30)	Relation between corrosion rate (experimental and calculated) vs. number of droplets at 40 °C, %water=0.05.	85

Figure (4-31)	Relation between corrosion rate (experimental and calculated) vs. number of droplets at 40 °C, %water=0.1.	85
Figure (4-32)	Relation between corrosion rate (experimental and calculated) vs. number of droplets at 40 °C, %water=0.2.	86
Figure (4-33)	Relation between corrosion rate (experimental and calculated) vs. number of droplets at 25 °C, %water=0.05.	86
Figure (4-34)	Relation between corrosion rate (experimental and calculated) vs. number of droplets at 25 °C, %water=0.15.	87
Figure (4-35)	Relation between corrosion rate (experimental and calculated) vs. number of droplets at 25 °C, %water=0.3.	87
Figure (4-36)	Vortex formation and circulation pattern in an agitated tank	91
Figure(B-1)	Relation between log Sauter mean diameter and log Re at 40°C, %water=0.01.	B-1
Figure(B-2)	Relation between log Sauter mean diameter and log Re at 40°C, %water=0.05.	B-1
Figure(B-3)	Relation between log Sauter mean diameter and log Re at 40°C, %water=0. 1.	B-2
Figure(B-4)	Relation between log Sauter mean diameter and log Re at 40°C, %water=0.2.	B-2

Figure(B-5)	Relation between log Sauter mean diameter and log Re at 25 ⁰ C, %water=0.05.	B-3
Figure(B-6)	Relation between log Sauter mean diameter and log Re at 25 ⁰ C, %water=0.15.	B-3
Figure(B-7)	Relation between log Sauter mean diameter and log Re at 25 ⁰ C, %water=0.3.	B-4
Figure(B-8)	Relation between corrosion rate(experimental and calculated) vs. Sautere mean diameter at 40 ⁰ C, %water=0.01.	B-4
Figure(B-9)	Relation between corrosion rate(experimental and calculated) vs. Sautere mean diameter at 40 ⁰ C, %water=0.05.	B-5
Figure(B-10)	Relation between corrosion rate(experimental and calculated) vs. Sautere mean diameter at 40 ⁰ C, %water=0. 1.	B-5
Figure(B-11)	Relation between corrosion rate(experimental and calculated) vs. Sautere mean diameter at 40 ⁰ C, %water=0.2.	B-6
Figure(B-12)	Relation between corrosion rate(experimental and calculated) vs. Sautere mean diameter at 25 ⁰ C, %water=0.05.	B-6
Figure(B-13)	Relation between corrosion rate(experimental and calculated) vs. Sautere mean diameter at 25 ⁰ C, %water=0.15.	B-7

Figure(B-14) Relation between corrosion rate(experimental
and calculated) vs. Sautere mean diameter
at 25⁰C, %water=0.3.

B-7

CHAPTER ONE

INTRODUCTION

1.1 Introduction

The word corrosion comes from the Latin corrode- to gnaw away ⁽¹⁾. It is as old as earth, but it has been known by different means. Corrosion is known commonly as rust, undesirable phenomena which destroys the luster and duty of objects and shortens their life. Corrosion since ancient times has affected not only the quality of daily lives of people, but also their technical progress. There is a historical record of observations of corrosion by several writers ⁽²⁾.

The serious consequences of corrosion process have become a problem of worldwide significance. In addition to our every day encounters with form of degradation, corrosion causes plant to shutdown, loss of most valuable resources, loss or contamination of product, reduction in efficiency, lost maintenance and expensive overdesign, it also jeopardizes safety and inhibits technological process ⁽³⁾.

Hardly a citizen may be found who does not; either directly by losses of personal possessions or indirectly by increased prices passed along by industry, bears some of the cost of this tremendous waste. There is evidently not a single branch of industry in which the necessity for protecting metals from corrosion does not arise. More precisely, in indirect as well as in direct ways, everyone and every industry pay for the cost of corrosion.

The degree of corrosion involved may be very slight, such as pitting penetration of a washer or a tube, but the consequences are large. Furthermore, surface oxidation of an electrical contact may cause failure of expensive sophisticated equipment leading to disastrous effects. Thus, the plague of corrosion, caused by reactions at small localized sites on the surface of the material, not only results in the loss of metal itself, but to a

much larger degree in the decay of metal structures and equipment. Generally it represents a loss of greater intrinsic value in the form of more than few human lives and vast sums of money every year.

Modern science and engineering are intimately concerned with corrosion and its effect. The materials scientist is constantly with searching for improvements in the anticorrosive quality in materials; the design engineer is seeking to understand the profound significance of corrosion on his design; and the maintenance engineer is endeavoring to combat it ⁽¹⁾.

Corrosion is the destructive attack of a metal by chemical or electrochemical reaction with its environment ⁽⁴⁾.

The multidisciplinary aspects of corrosion problems combined with the distributed responsibilities associated with such problems only increase the complexity of the subject ⁽³⁾.

Deterioration by physical causes is not called corrosion, but is described as erosion, galling, or wear. In some instance, chemical attack accompanied physical deterioration as described by the terms: corrosion-erosion, corrosion-wear, or fretting corrosion. Non metals are not included in present definition. Plastic may swell or crack, wood may split or decay, granite may erode and Portland cement may leach away. Therefore the term corrosion is presently restricted to chemical attack on metals.

Rusting applies to the corrosion of iron or iron-base with formation of corrosion products consisting largely of hydrous ferric oxides. Nonferrous metals therefore corrode but do not rust ⁽⁴⁾.

Corrosion has been classified in many different ways. One method divides corrosion into low- temperature and high- temperature corrosion. Another separates corrosion into direct combination (or oxidation) and electrochemical corrosion. The preferred classification is

1. Wet corrosion.

2. Dry corrosion.

Wet corrosion occurs when aqueous phase is present. This usually involves aqueous solution or electrolytes and accounts for greatest amount of corrosion by far. A common example is corrosion of steel by water. Dry corrosion occurs in absence of liquid or above the dew point of environment. Vapors and gases are usually the corrodents. Dry corrosion is most often associated with high temperatures. An example is attack on steel by furnace gases.

The presence of even small amount of moisture could change the corrosion picture completely. Dry chlorine is practically non corrosive to ordinary steel, but moist chlorine, or chlorine dissolved in water, is extremely corrosive and attacks most of the common metals and alloys. The reverse is true for titanium; dry chlorine gas is more corrosive than wet chlorine⁽⁵⁾.

Corrosion takes place according to the phase flow of the material, e.g. gas/vapor, liquid or solid. Two phase flow is generally understood as being a simultaneous flow of different immiscible phases separated by an infinitesimal thin interface. Phases are identified as "homogeneous" parts of the fluid for which unique local state and transport properties can be defined. Two phase flow is a long relevance for many scientific technical disciplines ranging from environmental research to the modeling of normal operation or accident conditions in nuclear, chemical, or process engineering installation. For a long time, the analysis of two phase flow process was limited to mostly empirical correlations or to largely simplified engineering models and therefore, two phase flow was considered as a rather 'dirty' branch of fluid dynamics. This situation has changed significantly (during the last three decades) when a large effort was spent for analysis of two phase flow methods. Much of this work was stimulated by the specific requirements for

the safety analysis of pressurized water reactors which for obvious reasons, relies largely on the prediction capability of computer codes for complex two phase flow and heat transfer process.

The petroleum industry contains a wide variety of corrosive environments. For example, oilfield are situated in tropical area where high humidity, salt bearing winds and air borne sand take the toll of structures and equipment. Costly pipelines convey the crude oil- often itself actively corrosive toward iron and steel – to long distance, either to refineries or to coastal installation where ocean – going tankers may be loaded via a submarine pipeline. In the refineries, the vast quantities of cooling water required for their operation, often necessitate the use of sea water, so that intake lines, condensers and cooler all require special protection against corrosive attack. Finally, the refined products must be distributed giving no rise to special corrosion problems in ocean going tankers and underground pipeline⁽¹⁾.

Nearly all corrosion problems which occur in oil field production operation are due to the presence of water. In order to corrode, the metal surface must be in contact with water phase. For example, if a well produces at a high oil to water ratio. Very little corrosion is likely to occur because the water is mixed with oil as an oil external emulsion. On the other hand, in low oil to water ratio wells, corrosion occurs because free water contacts the metal surface. Corrosion in the presence of water depends on electrochemical processes⁽⁶⁾.

1.2 Aim of Project

1. studying the effect of the two phase flow on corrosion by studying the effect of the Weber number , Reynold number and the droplets formed through the agitation and their mean diameter (Sauter mean diameter) by using mixing of two phase (water – kerosene).

2. Studying the effect of temperature by using data of two thesis at different temperatures (25 and 40 °C).
3. studying the effect of placement of the specimens. The placement used in this study near the wall and in the middle of the agitation vessel.

CHAPTER TWO

CORROSION

2.1 Corrosion under Two Phase Flow

Corrosion has been defined as the undesirable deterioration of a metal or alloy, i.e. an interaction of the metal with its environment that adversely affects those properties of the metal that are to be preserved. This definition- which will be referred to as the deterioration definition- is also applicable to non- metallic material such as glass, concrete, etc. and embodies the concept that corrosion is always deleterious⁽⁷⁾.

Corrosion represents the reverse of the process by which metal is produced from the ore form in which it exists naturally, such as , oxide, sulphide, chloride, etc. As a very broad generalization it can be said that the more difficult it has been to win the metal from its natural form, the greater will be its tendency to return to that form by corroding, but the rate of return will of course depend upon the environment⁽⁸⁾.

Since metals have a high electric conductivity, their corrosion is usually of an electrochemical nature. Of all type of destruction of structural materials, corrosion of metals draws the greatest amount of attention. Hence, where no particular reference is made to material, it is to be normally understood that a metal is being attacked ⁽¹⁾.

There are four necessary components of a differential corrosion cell⁽⁹⁾;

1. There must be an anode.
2. There must be a cathode.
3. There must be a metallic electrically connecting the anode and cathode.
4. The anode and cathode must be immersed in an electrically conductive electrolyte.

In the petroleum industry, mixtures of oil and water are transported over long distance in large-diameter pipelines. The presence of free water in pipeline may cause internal corrosion of the pipe walls. Corrosive gases such as carbon dioxide (CO_2) and hydrogen sulfide (H_2S) are also commonly presented in these systems. These gases dissolve into the water phase, which may cause internal corrosion in the pipelines. Typically at low water cuts (content) and high velocities this is not an issue as all the water is entrained by the following oil. As the water cut increases, water "break-out" may occur, leading to segregated flow of separate layers of water and oil phases. Therefore, the possibility of corrosion is high where the water phase wets the pipe walls (typically at the bottom)⁽¹⁶⁾.

In 1975 ⁽¹⁷⁾ published the first research paper on water entrainment. They proposed a simplified model for predicting the critical velocity of the flowing oil phase required to sweep out settled water. However, their model is suitable primarily for very low water cut situations. At high water cut, the model underestimates the critical velocity without considering the coalescence of water droplets. Since then, some efforts on this topic by a few researchers were implemented to establish empirical prediction models. However, no extensive experimental research and mechanistic modeling was involved. (1987) pointed out that some oils could carry water up to 20% water cut at velocities larger than (1 m/s) ⁽¹⁸⁾. From the original experiments, (1993) declared a binary water-wetting prediction factor suggesting that oil-wetting will occur only for water cuts less than 30% and velocities larger than 1 m/s, when all water can be entrained in to oil phase⁽¹⁹⁾. (1993) claimed that three phase wetting (oil, intermittent and water wettings) could exist. They estimated that below 30% water cut the tubing will be oil-wet; from 30-50%, intermittent water wetting occurs, and over 50% the tubing is water wetting⁽²⁰⁾. Obviously, they neglected or oversimplified the effect of the

properties of the oil and water phase, the flow regime and the flow geometry. Furthermore, field experience suggests that in some cases corrosion was obtained at water cuts as low as 2%, while no corrosion was obtained for water cuts high as 50%. (2001) updated the original empirical model (1993) and proposed a new empirical model using an analysis based on the emulsion breakpoint approach ⁽²¹⁾. This was a major step forward from the original model, however, while agreeing reasonably well with the specific pool of field cases used for its calibration, the new model remains an empirical correlation built on limited field data with an uncertain potential for extrapolation. More importantly, this model does not consider the effect of pipe diameter, physical and chemical properties of oil phase, flow regime and system temperature on the critical velocity of the flowing oil phase required for entrainment.

To understand the mechanism of water entrainment in the oil-water pipe flows, it is necessary to look closer into different flow regimes that occur. The main difficulties in understanding and modeling of the behavior of oil-water flows arise from the existence of the interfaces between the phases. The internal structures of two-phase flow can be best described by the flow patterns. The momentum and mass transfer mechanisms between the two phases significantly depend on the flow patterns. Also, flow patterns can indicate the phase wetting the pipe wall, position of the phases and the degree of mixing during the flow. A few studies are dedicated to flow of two immiscible liquids such as water and oil. However, it should be pointed out that most of these studies focused on the macroscopic phenomena related to flow structure, such as flow regimes and flow characteristics of two immiscible liquids in the pipelines. Less attention and effort was allocated to investigating the interaction between liquids and pipe wall and the phase

wetting issue, which is very important for corrosion engineers and helps them to determine the possibility of internal corrosion in the pipeline ⁽¹⁶⁾.

There are a variety of two – phase flows depending on combination of two phases as well as on interface structures. Two phase mixture are characterized by the existence of one or several interfaces and discontinuities at the interface. It is easy to classify two – phase mixtures according to combinations of two – phases since in standard conditions we have only three states of matters and at most four, namely, solid, liquid and gas phases and possible plasma. Therefore, we have ⁽²²⁾:

- Gas – Solid mixture.
- Gas – Liquid mixture.
- Liquid – Solid mixture.
- Immiscible – Liquid mixture.

The large number of flows encountered in chemical engineering are a mixture of phases. Physical phases of matter are gas, liquid, and solid, but the concept of phase in a multiphase flow system is applied in a broader sense. In multiphase flow, a phase can be defined as an identifiable class of material that has a particular inertial response to and interaction with the flow and the potential field in which it is immersed. For example, different – sizes solid particles of the same material can be treated as different phases because each collection of particles with the same size will have a similar dynamical response to the flow field.

Multiphase flow can be classified by the following regimes, grouped into four categories⁽²²⁾:

- Gas – liquid or liquid – liquid flows.

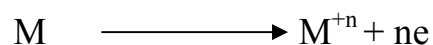
- Bubbly flow: discrete gaseous or fluid bubbles in a continuous fluid.
- Droplet flow: discrete fluid droplets in a continuous fluid.
- Slug flow: large bubbles in a continuous fluid.

Stratified/ free surface flow: immiscible fluids separated by a clearly – defined interface.

2.2 Oxidation and Reduction

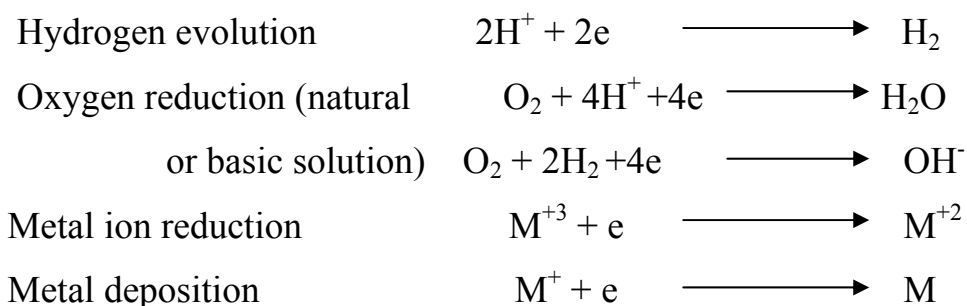
An oxidation or anodic reaction is indicated by an increase in valence or a production of electron⁽⁵⁾. The oxidation reaction causes the actual metal loss⁽⁹⁾. A decrease in valence charge or the consumption of electrons signifies as a reduction or cathodic reaction. The reduction must be present to consume the electrons liberated by the oxidation reaction, maintaining charge neutrality. Oxidation and reduction are electrochemical reactions which are necessary for corrosion to occur ⁽⁹⁾. Both reactions must occur simultaneously and at the same rate on the metal surface. If this was not true, the metal would spontaneously become electrically charged, which is clearly impossible. This leads to one of the most important basic principles of corrosion. During metallic corrosion, the rate of oxidation equals the rate of reduction (in terms of electron production and consumption).

Corrosion can be classified into a few generalized reactions. It is obvious that the anodic reaction in every corrosion is the oxidation of a metal to its ion. This can be written in a general form:



In each case the number of electrons produced equal the valence of ion.

There are several different cathodic reactions which are frequently encountered in metallic corrosion. The most common cathodic reactions are:



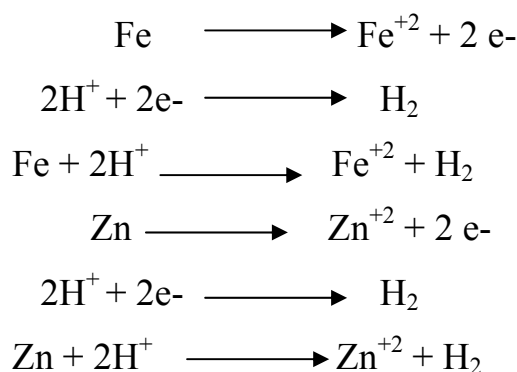
Hydrogen evolution is a common cathodic reaction since acid or acidic media are frequently encountered. Oxygen reduction is very common. Since any aqueous solution in contact with air is capable of producing this reaction. Metal ion reduction and metal deposition are less common reaction and are most frequently found in chemical process streams. All of the above reactions are quite similar - they consume electrons⁽⁵⁾.

2.3 Types of Corrosion

2.3.1 Uniform Corrosion

Uniform corrosion is characterized by corrosion attack proceeding evenly over the entire surface area or large fraction of the total area. General thinning takes place until failure⁽³⁾.

Aqueous corrosion of iron (Fe) in H_2SO_4 solution and of Zn in diluted H_2SO_4 solution are examples of uniform attack. Since Fe and Zn dissolve (oxidize) at a uniform rate according to the following anodic and cathodic reaction, respectively⁽¹⁰⁾.



The cathodic reaction is the common hydrogen evolution process.

Atmospheric corrosion of a steel structure is also a common example of uniform corrosion, which is manifested as brown – color corrosion layer on the exposed steel surface. This layer is ferric hydroxide compound known as rust⁽¹⁰⁾.

However, uniform corrosion is relatively easily measured and predicted, making disastrous failures relatively rare. In many cases, it is objectable only from an appearance standpoint. The breakdown of protective coating system on structures often leads to this form of corrosion. Surface type can be indicated in the protective coating system, however, should be examined closely for more advanced attack. Dulling of bright or polished surface, etching by acid cleaners, or oxidation of steel are examples of surface corrosion. Corrosion–resistance alloy and stainless steel can become tarnished or oxidized in corrosive environment. If surface corrosion is permitted to continue, the surface may become rough, and surface corrosion can lead to more serious type of corrosion⁽³⁾.

Uniform corrosion can be prevented or reduced by⁽⁵⁾ ;

1. Proper material, including coating.
2. Inhibitors.
3. Cathodic protection.

2.3.2 *Galvanic Corrosion*

Galvanic corrosion is an electrochemical corrosion. It is due to a potential difference between two different metals connected through a circuit for current flow to occur from more active metal (more negative potential) to more noble metal (more positive potential) ⁽¹⁰⁾.

The less resistance metal becomes anodic and the more resistance metal cathodic. Usually the cathodic or cathodic metal corrodes very little in this type of couple ⁽⁵⁾.

Galvanic corrosion occurs when dissimilar materials are brought into contact in the presence of an electrolyte. Such damage can also occur between metals and alloys and other conducting materials such as carbon or graphite. An electrochemical cell is set up due to differences in corrosion potential of the dissimilar materials ⁽³⁾.

A potential difference usually exists between two dissimilar metals when they are immersed in a corrosive or conductive solution. If these metals are placed in contact (or otherwise electrically connected), this potential difference produces electron flow between them. Corrosion of the less corrosion-resistant metal is usually increased and attack of the more resistant material is decreased, as compared with the behavior of these metals when they are not in contact ⁽⁵⁾.

In selecting two metals or two alloys for galvanic coupling, both metals should have similar potential or be close to each other in series in order to suppress galvanic corrosion. For example, Fe-Cr or Cu-Sn (bronze) couplings develop a very small potential difference since they are close to each other in their respective standard potential series. The closer the standard potential the weaker the galvanic effect; otherwise, the galvanic effect is enhanced ⁽⁹⁾.

2.3.3 *Pitting Corrosion*

Pitting is a form of extremely localized attack that results in holes in the metal. These holes may be small or large in diameter, but in most cases they are relatively small. Pits are sometimes isolated or so close together that they look like a rough surface. Generally a pit may be described as a cavity or hole with the surface diameter about the same or less than the depth.

Pitting is considered to be more dangerous than uniform corrosion damage because it is more difficult to detect or predict, and to design against. Corrosion products often cover the pit. It is one of the most destructive and insidious forms of corrosion.

A small narrow pit with minimal overall metal loss can lead to the failure of an entire engineering system ⁽³⁾.

Pits usually grow in the direction of gravity. Most pits develop and grow downward from horizontal surface. Lesser numbers start on vertical surface, and only rarely do pits grow upward from the bottom of the horizontal surface.

Pitting corrosion can produce pits with their mouth open (uncovered) or covered with a semi permeable membrane of corrosion products ⁽³⁾.

It is difficult to measure quantitatively and compare the extent of pitting because of varying depths and numbers of pits that may occur under identical conditions. Sometimes the pits require a long time - several months or year- to show up in actual service. Pitting is particularly vicious because it is a localized and intense form of corrosion, and failures often occur with extreme suddenness ⁽⁵⁾.

Materials that show pitting, or tendencies to pit, during corrosion test should not be used to build the plant or equipment under consideration. Some materials are more resistance to pitting than others. The best procedure is to use materials that are known not to pit in the environment under consideration.

2.3.4 *Crevice Corrosion*

Intensive localized corrosion frequently occurs within crevices and other shielded area on metal surface exposed to corrosives. This type of attack is usually associated with small volume of stagnant solution caused by holes,

gasket surface, lap joints, surface deposits, and crevice under bolt and rivet heads⁽⁵⁾.

Crevice corrosion is similar to pitting corrosion after its initiation stage in a stagnant electrolyte. The problem of crevice corrosion can be eliminated or reduced using proper sealants and protective coatings⁽¹⁰⁾.

This is a case for illustrating the effects of nonmetallic material (gasket, rubber, concrete, wood, plastic and the like) in contact with a surface metal or alloy exposed to an electrolytes (stagnant water). For instance, crevice attack can cut a stainless steel sheet by placing a stretched rubber band around it in seawater. Thus, metal dissolution occurs in the area of contact between the alloy and rubber band⁽⁵⁾.

2.3.5 Erosion Corrosion

Erosion corrosion is the acceleration or increase in rate of deterioration or attack on a metal because of relative movement between a corrosion fluid and the metal surface. Generally this movement is quite rapid, and mechanical wear effects or abrasion are involved. Metal is removed from the surface as dissolved ions, or it forms solid corrosion products that are mechanically swept from the metal surface. Sometimes movement of the environment decreases corrosion, particularly when localized attack occurs under stagnant conditions, corrosion decreases and thus cannot be considered as erosion corrosion.

Grooves, gullies, rounded edges, and waves on the surface usually indicating directionality characterizing this form of damage⁽³⁾.

The most severe erosion corrosion problems occur under conditions of disturbed turbulent flow at sudden changes in the flow system geometry, such as bends, heat exchanger-tube inlets, orifice plates, valves, fittings, and turbo-machinery including pumps, compressors, turbines, and propellers.

2.4 Polarization

Electrode reactions are assumed to induce deviations from equilibrium due to the passage of an electrical current through an electrochemical cell causing a change in the working electrode potential. This electrochemical phenomenon is referred to as polarization η . In this process, the deviation from equilibrium causes an electrical potential difference between the polarized and the equilibrium (unpolarized) electrode potential known as overpotential⁽¹⁰⁾.

There are three possible components: - activation, concentration, resistance polarization and combined polarization⁽¹¹⁾.

2.4.1 Activation polarization

Activation polarization refers to electrochemical reactions that are controlled by a slow step in the reaction sequence. This slow step during hydrogen evolution might be the electron transfer step or the formation of hydrogen molecules. The relation between reaction rate and overvoltage for activation polarization is :

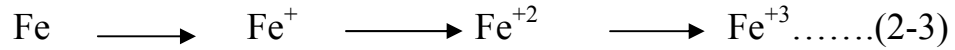
$$\eta_a = \pm \beta \log i/i_o \dots\dots\dots (2-1)$$

Where η_a is overvoltage, β is a constant, and i is the rate of oxidation or reduction in terms of current density. Equation (2-1) is called Tafel equation, and β is frequently termed " β slop" or Tafel constant⁽⁵⁾.

In general, the anodic metal undergoes a succession of reaction steps prior to dissolve in the electrolyte. This succession is hypothetically shown by the following idealized metal oxidation reactions during activation polarization



This succession indicates that the metal M loses +z electron on its surface and eventually the metal cation M^{+z} goes into solution. If the metal is silver undergoing oxidation, then the cation is just Ag^+ . For iron, the succession may be



For hydrogen evolution (fig (2-1)) which can be used to explain the succession of the reaction steps that may take place after the hydrogen cations are adsorbed (attached) on the electrode surface. Hence, the possible reaction steps are



Thus, only one step in equation (2-2) and one in equation (2-4) controls the charge transfer for activation polarization. For instance, the formation of hydrogen gas bubbles on the metal electrode surface is the last step in the succession of reactions and eventually, the bubbles move to the surface of the electrolyte where they burst ⁽¹⁰⁾.

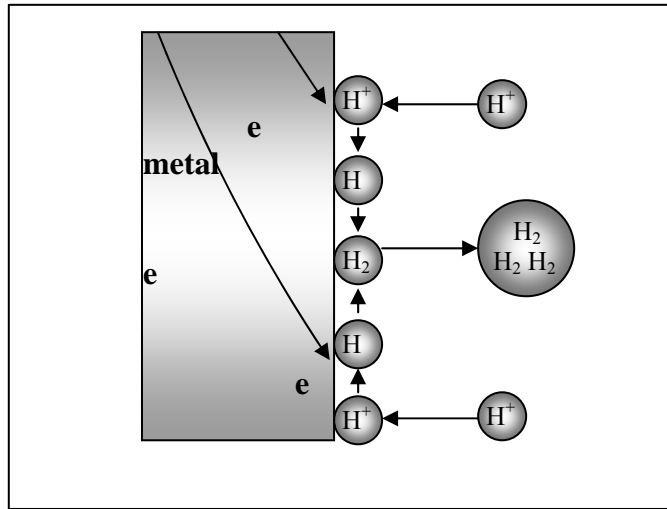


Figure (2-1)Hydrogen- reduction reaction under activation polarization ⁽⁵⁾.

According to the model in figure (2-1), the metal oxidation process can be represented by the following redox **stoichiometric reaction** $M + 2H = M^{+Z} + H_2$. On the other hand, if this reaction is reversed, then the metal M^{+Z} cations in solution, specifically at the electrode/electrolyte interface, are deposited (plated) on the metal electrode. This is possible since electrons in the solution are supplied to the electrode surface ⁽¹⁰⁾.

2.4.2 Concentration Polarization

Concentration polarization refers to electrochemical reactions which are controlled by the diffusion in the electrolyte. This is illustrated in figure (2-2) for the case of hydrogen evolution.

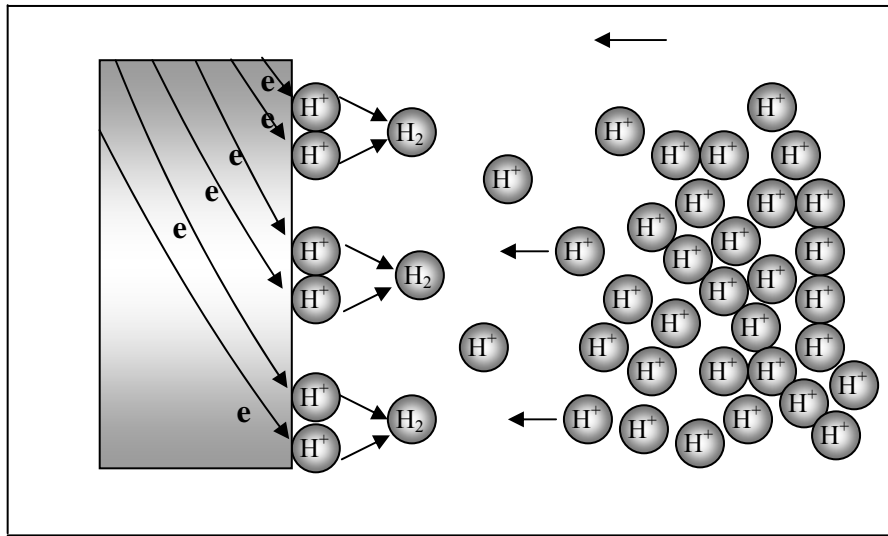


Figure (2-2) Concentration polarization during hydrogen reduction ⁽⁵⁾.

Here, the number of hydrogen ions in solution are quite small, and the reduction rate is controlled by the diffusion of hydrogen ions to the metal surface. In this case the reduction rate is controlled by processes occurring within the bulk solution rather than at the metal surface ⁽⁵⁾.

If the hydrogen is made cathode, whose activity of hydrogen ion is represented by (H^+) , then the potential E_1 , in absence of external current, is given by the Nernst equation at 25 °C

$$E_1 = 0.0592 \log (H^+) \dots\dots\dots (2-5)$$

When current flows, hydrogen is liberated on the electrode, thereby decreasing surface concentration of hydrogen ions to an activity $(H^+)_s$. The potential E_2 of the electrode at 25 °C now becomes:

$$E_2 = 0.0592 \log (H^+)_s \dots\dots\dots (2-6)$$

Since $(H^+)_s$ is less than (H^+) , the potential of the polarized cathode is less noble or more active than in the absence of external current. The difference of potential, $E_1 - E_2$, know as the *concentration polarization*, is equal to ⁽⁴⁾

$$E_2 - E_1 = 0.0592 \log ((H^+) / (H^+)_s) \dots\dots\dots (2-7)$$

The larger the current, the smaller is the surface concentration of hydrogen ion, or the smaller is $(H^+)_s$; therefore the larger is the corresponding polarization. Infinite concentration polarization is approached when $(H^+)_s$ approach zero at the electrode surface; the corresponding current density producing this limiting lower value of $(H^+)_s$ is called the *limiting current density* which can be evaluated from the expression⁽⁴⁾

$$i_L = DnFC / \delta t \quad \dots\dots\dots (2-8)$$

Where D is the diffusion coefficient for the ion being reduced, n is the number of electrons, F is the Faraday number (96487 C/eq), δ is the thickness of the stagnant layer of electrolyte next to the electrode surface (about 0.05 cm in an unstirred solution), t is the transference number of all ions in solution except the ion being reduced (equal to unity if many other ions are present), and C is the concentration of diffusing ion in mole/liter. Since D for all ion at 25 °C in dilute solution, except for H^+ and OH^- , average about $1 \times 10^{-5} \text{ cm}^2/\text{s}$, the limiting current density is approximated by⁽⁴⁾:

$$i_L = 0.02 \text{ nC} \quad \dots\dots\dots (2-9)$$

For H^+ and OH^- , D equals 9.3×10^{-5} and $5.2 \times 10^{-5} \text{ cm}^2/\text{s}$, respectively (infinite dilution), so that the corresponding values of i_L are higher⁽⁴⁾.

2.4.3 Resistance Polarization

In discussing activation and concentration polarization, no account was taken of ohmic resistances. For some electrode reactions the effects of ohmic resistance can be very considerable. This is especially significant when the reaction itself or a complementary reaction produces films on the electrode surface. The total potential drop across such resistance is called *resistance polarization*, η_R .

The total polarization at an electrode is therefore the sum of three components, activation, concentration and resistance polarization:

$$\eta_{\text{total}} = \eta_A + \eta_C + \eta_R \quad \dots\dots\dots (2-10)$$

The effects of these forms of polarization are illustrated by the characteristics of hydrogen evolution and oxygen reductions that feature prominently in corrosion process ⁽¹¹⁾.

2.4.4 Combined Polarization

Both activation and concentration polarization usually occur at an electrode. At low reaction rates, activation polarization usually controls, while at higher reaction rates concentration polarization becomes controlling. The total polarization of an electrode is the sum of the contribution of activation polarization and concentration polarization

$$\eta_T = \eta^A + \eta^C \quad \dots\dots\dots (2-11)$$

During reduction process such as hydrogen evolution or oxygen reduction, concentration polarization becomes important as the reduction rate approaches the limiting diffusion current density. The overall reaction for activation process is given by⁽⁵⁾:

$$\eta_{\text{red}} = -\beta_c \log \frac{i}{i_o} + \frac{2.303RT}{nF} \log \left(1 - \frac{i}{i_L} \right) \quad \dots\dots\dots (2-12)$$

This case can be shown in figure 2.3 ⁽⁵⁾.

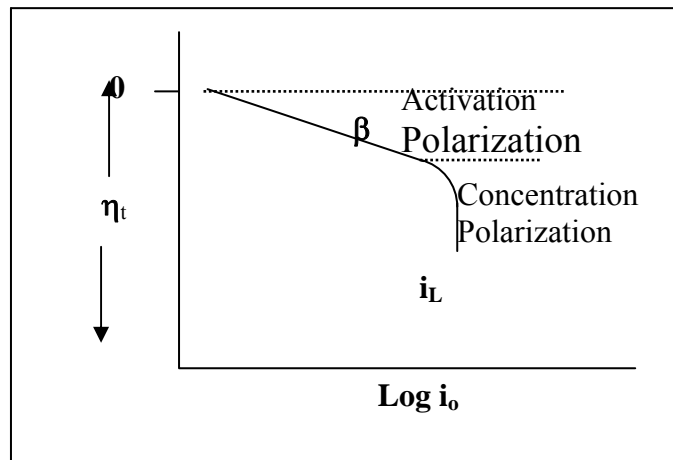


Figure (2.3) Combined Polarization curve ⁽⁵⁾.

In corrosion the resistance of the metallic path for charge transfer is negligible. Resistance overpotential η_R is determined by factors associated with the solution or with the metal surface ⁽⁷⁾.

The total polarization at a metal electrode then becomes as the algebraic sum of the three types described above ⁽¹²⁾.

2.5 Electrochemical Mechanism of Corrosion Rate

Corrosion is an electrochemical phenomenon comprised of anodic and cathodic half- cell processes. The rate of the anodic dissolution, e.g., of iron is occurring at the corroding surface. This balance can be altered by a vast number of changes in the experimental conditions, e.g., pH, ions formed, stirring, sample preparation, and contaminants in solution or in the iron electrode. A commonly used electrochemical method of studying corrosion is through polarization measurements. The main advantage of such a measurement is that it allows identification of the individual anodic and cathodic reactions taking place. In addition, the corrosion current (and hence the corrosion rate) can be determined by extrapolation of the cathodic or anodic Tafel lines on a polarization plot to the corrosion potential (E_{corr}). This is then inserted into Faraday's Law ⁽¹³⁾:

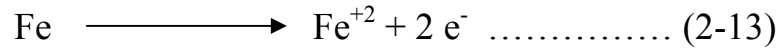
$$\text{Corrosion Rate (mols/s)} = I_{\text{corr}} / n F$$

Where, n = number of electrons involved in the reaction, and F (Faraday's constant)= 96487 A/s (C/eq). This is then converted to mass gain/ second by the relationship between moles and mass:

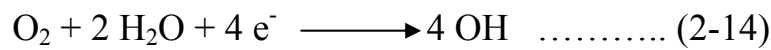
$$\text{Mass of sample} = \text{moles} \times \text{molecular mass of compound}$$

Meaningful data from this technique can only be obtained if the long period of polarization necessary to obtain steady state .Polarization curves dose not change the sample's surface properties. The reactions occurring at

the surface therefore are very significant. The anodic reaction is the formation of iron ions:



Because this is a rapid reaction in most environments, the overall reaction is controlled by the slower cathodic reactions. There are several possible cathodic processes, which may take place in nearly neutral solutions depending on the acidity and aeration of the solution. In aerated solutions, the cathodic reactions involve dissolved oxygen ⁽¹⁴⁾.



2.6 Factors Affecting Corrosion Rate

It is well known that the metals commonly used for the construction of industrial plants will corrode, and the rate at which corrosion takes place is of prime importance. Factors that influence the rate of attack are the conditions of the metal surface and the nature of the environment.

The effect of the different conditions is as follows⁽¹⁵⁾:

1. Type of metal: different metals corrode at different rates, generally speaking, ferrous metals corrode faster than non- ferrous metals.
2. Corrosion debris: corrosion will occur under deposits with the possibility of pitting attack.
3. Temperature: increases in temperature increase the corrosion rate.
4. pH: in the pH range (5.5-9.0), the corrosion rate of ferrous metals is fairly independent of pH.
5. Oxygen content: an increase in oxygen concentration generally gives an increase in corrosion.

6. Flow rate: increasing the aqueous phase flow rate gives better mass transport of oxygen and thus accelerates the corrosion rate.
7. Water type: the quality of the water is an important factor in determining the corrosion rates of metals.

2.7 Bubble Flow

Two phase bubbly flow has been one of the most fundamental flow fields occurring in many industrial applications. However, two – phase flow structure has not completely been understood and still in further investigations are needed. The main reason is the difficulty in conducting the measurement without disturbing the bubbly flow.

In most practical applications where two – phase bubbly flows occur, bubbles are seldom isolated or being spherical. However, due to the complexity of the general problem, most bubble dynamic studies have neglected bubble interaction and formation and have based their approach on isolated spherical bubble dynamics⁽²³⁾.

2.8 Characteristics of Agitation

Agitation is one of the oldest and simplest processes for speeding up mass transfer between two or more immiscible liquids. The forces acting in the agitation vessel break up one of the two liquids into small drops which are surrounded by the other liquid. These are then referred to as the disperse phase and the continuous phase respectively. The purpose of the agitation is to produce as large as possible an interfacial area between the two phases and hence small droplets. Information on the relationship between the physical properties of the two fluids, the conditions of agitation and the equipment geometry, on the one hand, and the resulting interfacial area between the phases on the other hand is therefore of considerable importance⁽²⁴⁾.

2.9 Agitation and mixing of liquids

Many processing operations depend for their sources on the effective agitation and mixing of fluids. Though often confused, agitation and mixing are not synonymous. Agitation refers to the induced motion of material in a specified way usually in circulatory pattern inside some sort of container ⁽²⁵⁾.

Mixing is the random distribution, into and through one another, of two or more initially separate phases. A single homogenous material, such as tankful of cold water, can be agitated, but it can not be mixed until some other material is added to it.

The term of mixing is applied to variety of operations, differing widely in the degree of homogeneity of the "mixed" material ⁽²⁵⁾.

2.9.1 Purpose of Agitation

There are a number of purposes for agitating fluids and some of these are briefly summarized ⁽²⁶⁾.

1. Blending of two miscible liquids, such as ethyl alcohol and water.
2. Dissolving solids in liquids, such as salt in water.
3. Dispersing a gas in liquid as fine bubble.
4. Suspending of fine solid particles in liquid.
5. Agitation of the fluid to increase heat transfer between the fluid and coil or jacket in the vessel wall.
6. Dispersing a second liquid, immiscible with the first, to form an emulsion or suspension of line drops.
7. Crystallization and emulsion.

2.9.2 Agitated vessels

Liquids are most often agitated in some kind of tank or vessel, usually cylindrical in form and with a vertical axis. The top of the vessel may be open to the air, more usually it is closed. The proportion of the tank vary widely, depending on the nature of the agitation problem. A standardized design such as that shown in Fig(3.1),however, is applicable in many situations. The tank bottom is rounded, not flat, to eliminate sharp corner or regions into which fluid currents would not penetrate. The liquid depth is approximately equal to the diameter of the tank⁽²⁷⁾.

Accessories such as inlet and outlet lines, coils, jackets, and wells thermometer or other temperature measuring devices are usually included.

The impellers cause the liquid to circulate through the vessel eventually return to the impeller. Baffles are often included to reduce tangential motion.

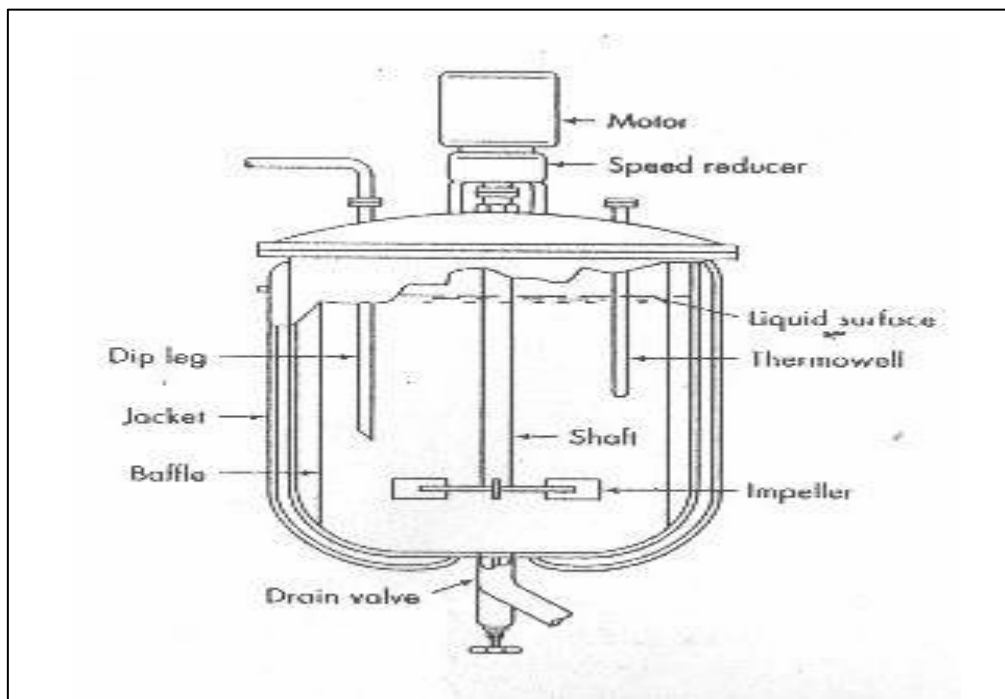


Figure (2.4) typical agitation process vessel⁽²⁶⁾.

2.9.3 Impellers

Impeller agitators are divided into two classes. Those that generate currents parallel with the axis of the impeller shaft are called axial flow impeller and those that generate currents in radial or tangential directions are called radial flow impellers.

The three main types of impellers for low-to moderate viscosity liquids are propellers, turbine, and high efficiency impellers. Each type includes many variations and subtypes, which are not considered here. For very viscous liquids, the most widely used impellers are helical impellers and anchor agitators⁽²⁵⁾.

2.9.4 Turbine

There are several types of agitation turbines commonly used fig. (3-2). The common type is a three bladed marine type propeller similar to propeller blade used in driving boats fig.(3-2.a). This type of flow pattern is called axial flow since the fluid flows axially down the center axis or propeller shaft and up on the sides of the tank⁽²⁵⁾.

Fig. (3-2.b) shows the simple straight blade turbine which pushes the liquid radially and tangentially with almost no vertical motion at the impeller. The currents generate travel outward to the vessel wall and then flow either upward or downward. Such impellers are sometimes called puddles. In process vessel they typically run at 20-150 rpm⁽²⁶⁾.

The disk turbine fig. (3-2.c) with multiple straight blades mounted on a horizontal disk like the straight blade impeller, creates zones of high shear rate; it is especially useful for dispersing gas in liquid⁽²⁷⁾.

The concave blade turbine CD-6 disk turbine fig. (3-2.d) is widely used for gas dispersion. A pitch blade turbine fig. (3.2-e) is used when good overall circulation is important ⁽²⁷⁾.

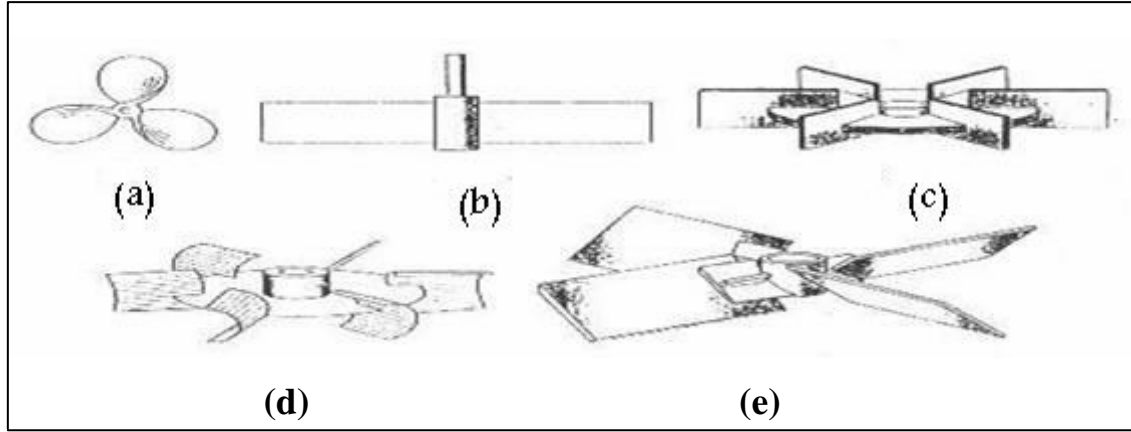


Figure (2.5) Types of turbine impellers ⁽²⁴⁾.

2.9.5 Standard turbine design

The designer of an agitated vessel has unusually large number of choices to make as to type and location of the impeller .The proportions of the vessel, the number and properties of the baffles, and so forth affect the circulation rate of the liquid, the velocity patterns, and the power consumed .As starting point for design in ordinary agitation problems., a turbine agitator of the type as shown in Fig. (2.6) is commonly used .Typical proportions are in table (2.1) :-

Table (2.1) design equations of agitator (cylinder) ⁽²⁶⁾ .

$\frac{D_a}{D_t} = \frac{1}{3}$,	$\frac{H}{D_t} = 1$,	$\frac{J}{D_t} = \frac{1}{12}$
$\frac{E}{D_t} = \frac{1}{3}$,	$\frac{w}{D_a} = \frac{1}{5}$,	$\frac{L}{D_a} = \frac{1}{4}$

Where:

D_a: diameter of impeller.

D_t: diameter of tank (cylinder).

E: distance from center of impeller to bottom of tank (cylinder).

H: height of tank (cylinder)

J: width of baffles

L: length of impeller

W: width of impeller

The number of the baffles is usually four, the number of the impeller blades ranges from (4-16) but it is generally (6-8).

Special situation may, of course, dictate different proportions from these listed above: it may be advantageous, for example, to place the agitator higher or lower in the tank, or a much deeper tank may be needed to achieve the desired process result. The listed standard proportions, nevertheless, are widely accepted and are the basis of many published correlation of agitator performance⁽²⁵⁾.

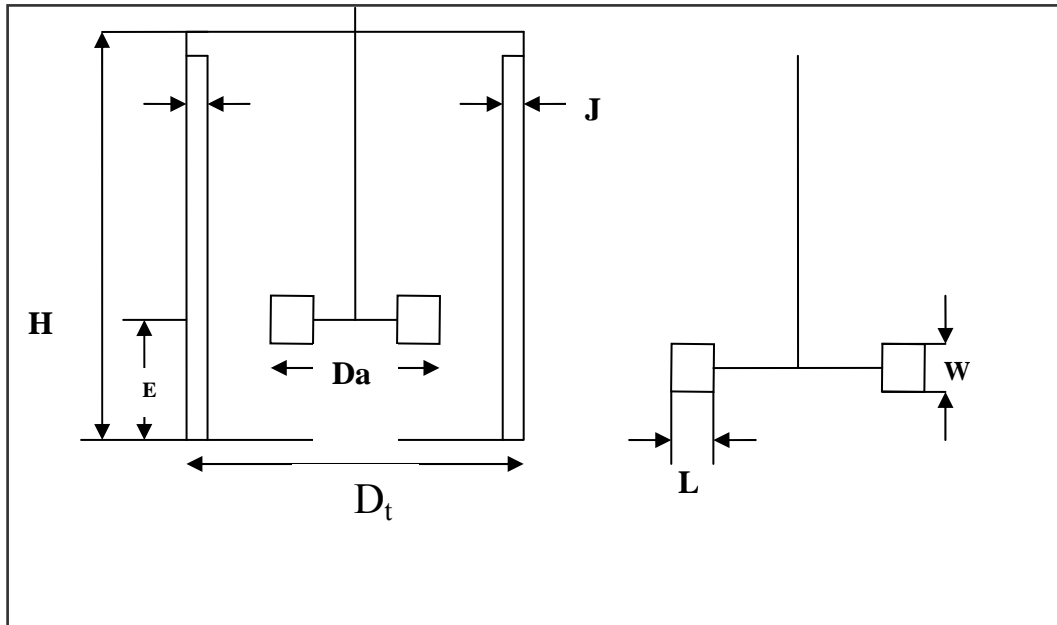


Figure (2.6) measurements of turbine ⁽²⁵⁾.

2.10 Phase Inversion of Liquid-Liquid Dispersions in Agitated Vessel

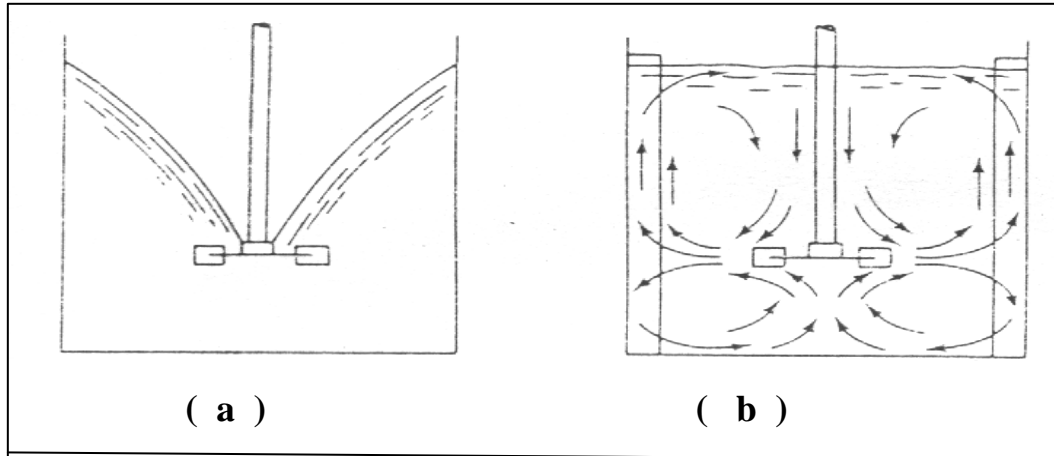
Liquid-liquid dispersions in agitated vessels are frequently used in the chemical industry for conducting operations such as solvent extraction and heterogeneous reactions. In liquid-liquid two-phase flow systems, usually consisting of an aqueous and an organic liquid. There are two general types of dispersions in which either oil drops are dispersed in a water phase (oil-in-water) or water drops are dispersed in an oil phase (water-in-oil). Phase inversion is defined as the phenomenon whereby the phases of a liquid-liquid dispersion interchange so that the dispersed phase spontaneously inverts to become the continuous phase and *vice versa*, under conditions that are determined by the system properties and operational parameters such as phase volume ratio and energy input. In general, for dispersions formed in agitated vessels phase inversion will take place at a critical impeller speed and for a certain dispersed phase fraction. Phase inversion can be obtained by either

increasing the dispersed phase volume fraction or increasing the agitation speed (or power input). In some chemical processes, such as solvent extraction in mixer-settlers, phase inversion can be undesirable because it can delay the settling process. On the other hand, phase inversion could be desirable in some operations, such as the preparation of water-borne dispersions of polymer resin⁽²⁸⁾.

Experimental studies reported in the literature, however, have indicated that phase inversion is affected not only by a number of physical and physicochemical parameters, but also by container geometry and the initial conditions of flow systems.

2.11 Flow pattern in agitation

The flow pattern in agitation tank depends upon the fluid properties, the geometry of the tank, type of baffles in the tank and the characterization of the liquid, especially its viscosity. If an agitator is mounted vertically in the center of tank with no baffles, a swirling flow patterns usually develop. Generally this is undesirable, because its resulting in excessive air entering and development of a large vortex and surging, especially at high speed. The turbine impellers drive the liquid radially against the wall, where it is divided, one portion flowing upward near the surface and back to the impeller, the other portion flowing downward fig(3.4)⁽²³⁾.



Figure(2.7) disk flat blade turbine .(a) without baffles .(b) with baffles. ⁽²³⁾

2.12 Mass Transfer to Suspension of Small Particles

Mass transfer from or to small suspended particles in an agitated solution occurs in a number of process application. In liquid phase hydrogenation, hydrogen diffuses from gas bubbles, through an organic liquid, and then to small suspended catalyst particles.

For a liquid-solid or liquid-liquid dispersion, increasing agitation over and above necessary to freely suspend very small particles has very little effect on the mass transfer coefficient k_L to the particle. When the particles in a mixing vessel are just completely suspended, turbulence force balance those due to gravity, and the mass transfer rates are the same as for particles freely moving under gravity.

When agitation power is increased beyond that needed for suspension of solid or liquid particles and the turbulence forces become larger than gravitational force equation (2. 16) should be used ⁽²⁶⁾:

$$k_i Sc^{2/3} = 0.13 \left(\frac{(p/v)u_c}{\rho_c^2} \right)^{1/4} \quad (2.16)$$

Where

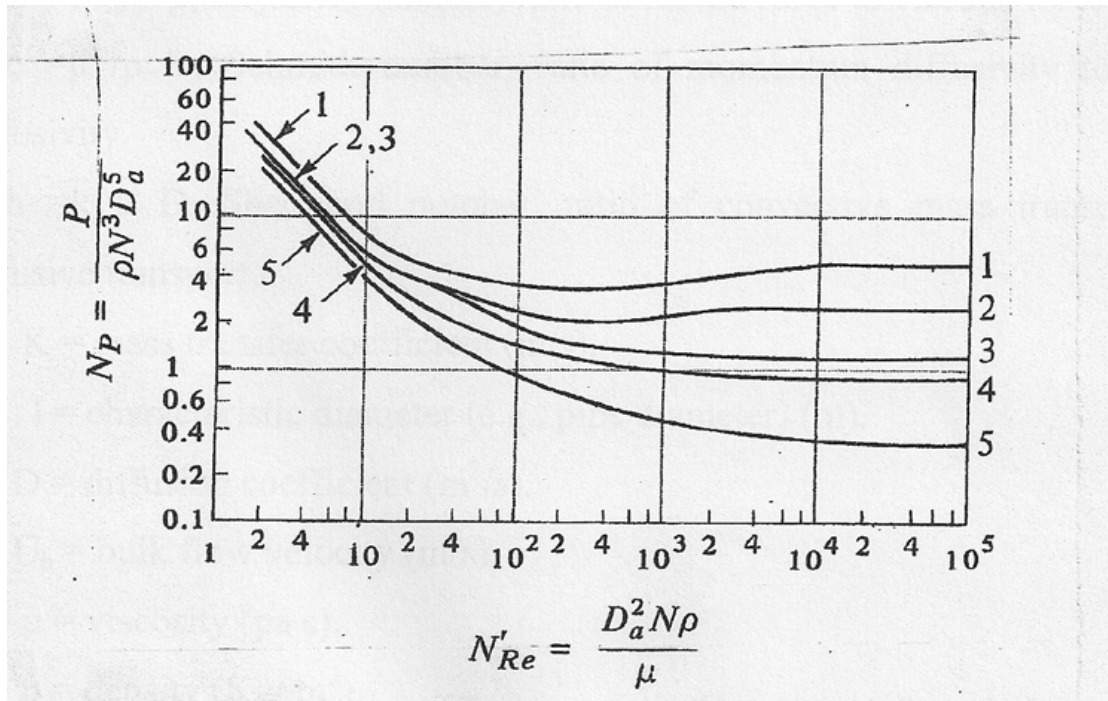
k_l = mass transfer coefficient (m/s).

Sc = Schmidt number (dimension less).

P/v = power input per unit volume estimated from fig (2.8).

μ_c = viscosity of continuous phase (poise).

ρ_c = density of continuous phase (Kg/m^3).



Figure(2.8) Power correlation for various impellers and baffles⁽²⁶⁾.

Curve 1. Flat six-blade turbine with disk: $D_a/W = 5$; four baffles each $D_t/J = 12$.

Curve 2. Flat six-blade open turbine ; $D_a/W = 8$; four baffles each $D_t/J = 12$.

Curve 3. Six-blade open turbine but blades at 45° ; $D_a/W = 8$; four baffles each $D_t/J = 12$.

Curve 4. Propeller ; pitch = $2D_a$: four baffles each $D_t/J = 10$; also holds for same propeller in angular off center position with no baffles.

Curve 5. . Propeller ; pitch = D_a : four baffles each $D_t/J = 10$; also holds for same propeller in angular off center position with no baffles.

When corrosion is controlled by the rate of dissolved oxygen mass transfer, the corrosion rate can be calculated by the application of well established mass transfer correlations of dimensionless groups. In general ⁽¹²⁾

$$Sh = \alpha Re^\lambda Sc^\gamma \dots\dots\dots (2.17)$$

Where:

$Re = l u_b \rho / \mu$, Reynolds number, ratio of inertia force to viscous force.

$Sc = \mu / \rho D$, Schmidt number, ratio of momentum diffusivity to mass diffusivity.

$Sh = k l / D$, Sherwood number, ratio of convective mass transport to diffusive transport.

K = mass transfer coefficient (m/s).

l = characteristic diameter (e.g., pipe diameter) (m).

D = diffusion coefficient (m^2/s).

U_b = bulk flow velocity (m/s).

μ = viscosity (pa s).

ρ = density (Kg/ m^3).

α, λ, γ = experimental constants.

After carefully analyzing the stratified flow data, a modified mass transfer correlation for stratified flow was identified⁽²⁹⁾:

$$Sh = 0.64 Re^{0.59} Sc^{0.33} \dots\dots\dots (2.18)$$

The liquid film height is used to compute Sherwood number and the pipe diameter is used to compute Reynolds number.

2.13 Two Ways Analysis of Variance

An experimental design is a plan for the orderly collection and analysis of data. The chief objective of a good designer is to obtain more information for less cost than normally can be obtained by traditional sampling methods.

Many investigators proceed to gather data under the assumption that statistical problems must be faced only when the task of analysis begins. The need for careful planning well in advance of a statistical study is as important as the details and specifications that must precede the construction of a house. In statistical study, the bad planning or no planning at all can lead to poor results or exorbitant costs, or both⁽³⁰⁾.

Often it is desirable to test hypotheses concerning two variables. These two variables may be referred to as row effects and column effects⁽³¹⁾.

Computational formulas:

Correction factor

$$C = \frac{T^2}{r.c} \quad (2.19)$$

Where,

r= the number of rows.

c= the number of columns.

Between Rows Sum of Squares.

$$SSR = \frac{\sum_{i=1}^r T_i^2}{c} - C \quad (2.20)$$

Between Columns Sum of Squares.

$$SSC = \frac{\sum_{j=1}^c T_j^2}{r} - C \quad (2.21)$$

Total Sum of Squares.

$$SST = \sum_{i=1}^r \sum_{j=1}^c x_{ij}^2 - C \quad (2.22)$$

Error Sum of Squares.

$$SSE = SST - SSR - SSC \quad (2.23)$$

$$MSC = \frac{SSC}{c - 1} \quad (2.24)$$

$$MSR = \frac{SSR}{r - 1} \quad (2.25)$$

$$MSE = \frac{SSE}{(r - 1)(c - 1)} \quad (2.26)$$

$$F_R = \frac{MSR}{MSE} \quad (2.27)$$

$$F_C = \frac{MSC}{MSE} \quad (2.28)$$

In testing hypotheses concerning two variables, it is possible to have more than one observation per cell ⁽³²⁾.

Computational formulas:

Correction factor

$$C = \frac{T^2}{r.c.n} \quad (2.29)$$

Where,

r= the number of rows.

c= the number of columns.

n= number of observation per cell and is the same for all cells.

Between Rows Sum of Squares.

$$SSR = \frac{\sum_{i=1}^r T_i^2}{c.n} - C \quad (2.30)$$

Between Columns Sum of Squares.

$$SSC = \frac{\sum_{j=1}^c T_j^2}{r.n} - C \quad (2.31)$$

Between Mean Sum of Squares.

$$SSM = \frac{\sum_{i=1}^r \sum_{j=1}^c x_{ij}^2}{n} - C \quad (2.32)$$

Interaction Sum of Squares.

$$SSI = SSM - SSR - SSC \quad (2.33)$$

Total sum of Squares.

$$SSI = \sum_{i=1}^r \sum_{j=1}^c \sum_{k=1}^n x_{ij}^2 - C \quad (2.34)$$

Error Sum of Squares.

$$SSE = SST - SSM \quad (2.35)$$

$$MSI = \frac{SSI}{(r-1)(c-1)} \quad (2.36)$$

$$MSE = \frac{SSE}{rc(n-1)} \quad (2.37)$$

$$F_I = \frac{MSI}{MSE} \quad (2.38)$$

Where MSC, MSR, F_C , F_R are as given before.

CHAPTER THREE

RESULTS AND CALCULATIONS

3.1 Introduction

Liquid-liquid dispersions in agitated vessels are frequently used in the chemical industry for conducting operations such as solvent extraction and heterogeneous reactions. In liquid-liquid two-phase flow systems, usually consisting of an aqueous and an organic liquid, there are two general types of dispersions in which either oil drops are dispersed in a water phase (oil-in-water) or water drops are dispersed in an oil phase (water-in-oil) .

The study was carried for the system liquid – liquid (water – kerosene) taking in consideration the following parameters: Reynold number, Weber number, Sauter mean diameter (d_{32}), interfacial area (a), number of droplets(n), number of droplet per unit volume(n/v), mass transfer coefficient (k), number of droplets striking the specimen.

The results and calculations of the parameters gained in this research were according to the laws and rules affecting each parameter.

3-2 Reynold number

Specific properties are the fluid densities, viscosity, temperatures, pressures, and volatility. These properties have been related in a dimensionless formula called the Reynolds Impeller Number defined here ⁽³³⁾:

$$Re = \frac{\rho \times D_a^2 \times N_I}{\mu} \quad (3.1)$$

Where:

D_a = Impeller diameter (m)

N_I = Rotational speed of the impeller (Rev/Second)

ρ = Fluid density(kg/m³)

μ = Fluid viscosity (kg/m.sec.)

Some observations regarding the Reynolds Impeller Number:

A) If ($Re \leq 10$), flow is laminar. If ($Re > 10000$), flow is turbulent, and between 10 and 10000 there is a transition range where both laminar and turbulent flow elements exist.

B) Doubling the impeller diameter will quadruple (Re). This follows, as the impeller will sweep an area four times larger when the diameter is doubled.

C) Temperatures and pressures are accounted in (Re) as they affect both density and viscosity. It is obvious that temperature affects the physical properties of the fluids, therefore two different temperatures (25 and 40 °C) were selected to identify the effect of temperature.

These factors are useful for sizing and selections of tanks, impellers, and the associated driving equipment.

Reynolds number can be calculated from equation below for multiphase (aqueous solution immiscible with kerosene)⁽³³⁾

$$Re = \frac{\rho_{mix} \times D_a^2 \times N_I}{\mu_{mix}} \quad (3.2)$$

Where:

D_a = Impeller diameter (m).

N_I = Rotational speed of the impeller (Rev/Second).

ρ_{mix} = Fluids (aqueous solution 0.1 N NaCl immiscible with kerosene) mixture density(kg/m³).

μ_{mix} = Fluids (aqueous solution 0.1 N NaCl immiscible with kerosene)

3-3 Weber number (We)

Weber number is the ratio of the flow kinetic energy at the impeller tip speed to surface tension stress based on impeller diameter(D_a)⁽³⁴⁾. It is an important dimensionless group.

Weber number can be calculated from equation below:

$$We = \frac{\rho_c \times (N_I)^2 \times D_a}{\sigma} \quad (3.3)$$

Where

We: weber number(dimensionless)

ρ_c : density of continuous phase(Kg/m³)

σ : interfacial tension(N/m).

D_a : Impeller diameter (m)

N_I : Rotational speed of the impeller (Rev./Second)

3.4 Sauter mean diameter

In a stirred tank the average drop size depends on a balance between breakup of large drops in regions of high shear and drop coalescence in regions of lower shear. Shear stress at the drop surface tends to deform the drop, and deformation is resisted by the interfacial tension and the viscosity of the dispersed phase.

Sauter diameter can be calculated from equation below⁽³⁵⁾:

$$\frac{d_{32}}{D} = 0.058 (1 + 5.4\Psi) \times We^{-0.6} \quad (3.4)$$

Where:

d_{32} : volume surface mean diameter of drops or bubbles (m).

D: Impeller diameter (m)

Ψ : volumetric fraction gas or liquid holdup in dispersion (dimensionless)

We: Weber number (dimensionless)

3-5 Number of Droplets

The number of droplets depend on water volume used and droplets size formed. It is clear that when water volume increases the number of droplets

are increased too. This is true up to a certain level of water. When water volume goes beyond this level, coalescence between droplets takes place resulting in lesser number of droplets. According to Attwan⁽³⁸⁾, the number of droplets increased in 5 and 15 % of water and decreased when the volume of water reached or exceeded 20 %^(38,39).

$$\text{Total number of droplets} = \text{volume of water} / \text{volume of drop} \quad (3.5)$$

Where

$$\text{Volume of droplet} = 4/3 \pi (\text{sauter mean diameter}/2)^3 \quad (3.6)$$

$$\text{Volume of water} = \Psi \times \text{Total volume of mixture} \quad (3.7)$$

It is well known that not all the droplets hits the specimen, but part of them. The number of these droplets can be known from the quantity of O₂ comes from kerosene to water to the specimen. Therefore, the number of droplets can be estimated from the transfer of O₂ and the units of gmd to the equivalent mol O₂ consumed, then divided by amount of O₂ in each droplet see table (3-1,2,3,4).

$$\text{Number of drops striking} = \text{Mole O}_2 \text{ consumed} / \text{Mole O}_2 \text{ in drops} \quad (3.8)$$

the specimen

Where

$$\text{Mole O}_2 \text{ consumed} = (\text{gmd} / \text{M.wt} / 2) \times (1/24 \times 3600) \times \pi \text{dl} \quad (3.9)$$

$$\text{Mole O}_2 \text{ in drops} = \text{Mole of O}_2 / \text{total number of droplet} \quad (3.10)$$

$$\text{Mole of O}_2 = \text{solubility} \times \text{total volume} \times \Psi / \text{M.wt. of O}_2 \quad (3.11)$$

Table (3-1) Total number of droplets at 25 °C . $\rho_{\text{water}} = 997.06 \text{ Kg/m}^3$,
 $\rho_{\text{kerosen.}} = 777.722 \text{ Kg/m}^3$, $\mu_{\text{water}} = 0.8937 \text{ cp}$, $\mu_{\text{kerosen}} = 2.5 \text{ cp}$. Impller diameter 9 cm

$\phi^{(36)}$	We	Re/rpm	$D_{32} \times 10^5$ (m)	a (m^{-1})	$n \times 10^{-11}$	$n/v \times 10^{-11}$
0.05	28927	11879(270)	1.4	21499	4.29	1.19
0.05	40632	14079(320)	1.14	26361	7.908	2.20
0.05	80351	19799(450)	0.756	39687	26.984	7.50
0.15	28927	13074(270)	1.99	45255	4.446	1.24
0.15	40632	15495(320)	1.62	55490	8.196	2.28
0.15	80351	21790(450)	1.08	83539	27.965	7.77
0.3	28927	15235(270)	2.88	62529	2.932	0.81
0.3	40632	18057(320)	2.35	76669	5.404	1.5

Table (3-2) Total number of droplets at 40 °C. $\rho_{\text{water.}}=992.25 \text{ Kg/m}^3$, $\rho_{\text{kerosen.}}=773.955 \text{ Kg/m}^3$, $\mu_{\text{water}}=0.656 \text{ cp}$, $\mu_{\text{kerosen}}=2.1\text{cp}$, Impeller diameter 8 cm.

ϕ^{37}	We	Re/rpm	$D_{32} \times 10^6$	$a(\text{m}^{-1})$	$n \times 10^{-12}$	$n/v \times 10^{-12}$
0.01	126360	23824(600)	4.25	14118	3.04	0.25
0.01	224640	31765(800)	3	19938	8.55	0.70
0.01	351000	39707(1000)	2.3	26060	19.1	1.55
0.01	505440	47648(1200)	1.85	32434	36.82	2.99
0.01	687960	55589(1400)	1.54	39024	64.14	5.21
0.05	126360	24957(600)	5.12	58582	8.68	0.71
0.05	224640	33276(800)	3.63	82735	24.45	1.99
0.05	351000	41596(1000)	2.77	108139	54.6	4.44
0.05	505440	49915(1200)	2.23	134586	105.24	8.56
0.05	687960	58234(1400)	1.85	161934	183.31	14.90
0.1	126360	26051(600)	6.21	96623	9.74	0.79
0.1	224640	34735(800)	4.4	136460	27.42	2.23
0.1	351000	43419(1000)	3.36	178360	61.24	4.98
0.1	505440	52102(1200)	2.7	221980	118.05	9.60
0.1	687960	60786(1400)	2.25	267086	205.63	16.72
0.2	126360	28910(600)	8.39	143076	7.9	0.64
0.2	224640	38547(800)	5.94	202066	22.26	1.81
0.2	351000	48184(1000)	4.54	264110	49.71	4.04
0.2	505440	57820(1200)	3.65	328702	95.82	7.79
0.2	687960	67457(1400)	3.03	395492	166.91	13.57

Table (3-3) The number of drops striking the specimen/ second at 25 °C

rpm ⁽³⁶⁾	% ⁽³⁶⁾	d ₃₂ X 10 ⁵	vol. of drop	g of O ₂	mol of O ₂	nx10 ⁻¹¹	mol of O ₂ in dropx10 ¹⁵	C.R _{Exp.} gmd ⁽²⁷⁾	O ₂ cons.X10 ⁷	no of drops str. x 10 ⁻⁹
270	0.05	1.4	3.38E-15	0.0041	0.000128	4.29	0.3	41.029	1.92	0.644
320	0.05	1.14	1.82E-15	0.0041	0.000128	7.908	0.16	44.991	2.11	1.302
450	0.05	0.756	5.31E-16	0.0041	0.000128	26.984	0.05	48.658	2.28	4.806
270	0.15	1.99	9.69E-15	0.013	0.000406	4.446	0.91	50.314	2.36	0.258
320	0.15	1.62	5.23E-15	0.013	0.000406	8.196	0.5	56.729	2.66	0.537
450	0.15	1.08	1.55E-15	0.013	0.000406	27.965	0.15	75.031	3.52	2.422
270	0.3	2.88	2.94E-14	0.024	0.00075	2.932	2.56	51.723	2.43	0.095
320	0.3	2.35	1.60E-14	0.024	0.00075	5.4044	1.39	67.515	3.17	0.228

Table (3-4) The number of drops striking the specimen/ second at 40 °C

rpm ⁽³⁷⁾	% ⁽³⁷⁾	d ₃₂ X 10 ⁶	vol. of drop	g of O ₂	mol of O ₂	nx 10 ⁻¹²	mol of O ₂ in dropx10 ¹⁸	C.R _{Exp.} gmd ⁽²⁸⁾	O ₂ cons.x10 ⁹	no of drops str..x 10 ⁻⁷
600	0.01	4.25	4.0174E- 17	0.000781	0.0000244	3.04	8.03	9.306	3.79	0.47
800	0.01	3	1.413E-17	0.000781	0.0000244	8.55	2.85	14.204	5.78	2.03
1000	0.01	2.3	6.3674E- 18	0.000781	0.0000244	19.1	1.28	19.102	7.78	6.09
1200	0.01	1.85	3.31355E- 18	0.000781	0.0000244	36.82	0.66	21.55	8.77	13.24
1400	0.01	1.54	1.91135E- 18	0.000781	0.0000244	64.14	0.38	29.87	12.16	31.96
600	0.05	5.12	7.02406E- 17	0.003904	0.000122	8.68	14.06	16.65	6.78	0.48
800	0.05	3.63	2.50322E- 17	0.003904	0.000122	24.45	4.99	20.08	8.17	1.64
1000	0.05	2.77	1.11229E- 17	0.003904	0.000122	54.6	2.23	24	9.77	4.37
1200	0.05	2.23	5.80354E- 18	0.003904	0.000122	105.24	1.16	25.9	10.54	9.09
1400	0.05	1.85	3.31355E- 18	0.003904	0.000122	183.31	0.67	32.816	13.36	20.07

Table (3-4) The number of drops striking the specimen/ second at 40 °C (continued)

rpm ⁽³⁷⁾	% ⁽³⁷⁾	d ₃₂ X 10 ⁶	vol. of drop	g of O ₂	mol of O ₂	nx 10 ⁻¹²	mol of O ₂ in dropx10 ¹⁸	C.R _{Exp.} gmd ⁽²⁸⁾	O ₂ cons.x10 ⁹	no of drops str..x 10 ⁻⁷
600	0.1	6.21	1.25329E-16	0.007808	0.000244	9.74	25.05	66.613	27.12	1.08
800	0.1	4.4	4.45796E-17	0.007808	0.000244	27.42	8.90	73.47	29.91	3.36
1000	0.1	3.36	1.98516E-17	0.007808	0.000244	61.24	3.98	79.48	32.35	8.12
1200	0.1	2.7	1.03008E-17	0.007808	0.000244	118.05	2.07	84.61	34.44	16.66
1400	0.1	2.25	5.96109E-18	0.007808	0.000244	205.63	1.19	95.63	38.93	32.81
600	0.2	8.39	3.09075E-16	0.015616	0.000488	7.9	61.77	74.26	30.23	0.49
800	0.2	5.94	1.09683E-16	0.015616	0.000488	22.26	21.92	77.16	31.41	1.43
1000	0.2	4.54	4.89718E-17	0.015616	0.000488	49.71	9.82	86.93	35.39	3.60
1200	0.2	3.65	2.54482E-17	0.015616	0.000488	95.82	5.09	93.76	38.17	7.49
1400	0.2	3.03	1.45582E-17	0.015616	0.000488	166.91	2.92	105.61	42.99	14.70

3-6 Mass transfer coefficient

Mass transfer coefficient is calculated according to equation (2-16) as shown in tables (3-7,8). This equation is applied to liquid-liquid dispersion and very small suspended particles ⁽²⁶⁾. Also, the mass transfer coefficient is calculated from average corrosion rates as shown in tables (3- 5, 6)

$$k_l Sc^{2/3} = 0.13 \left(\frac{(P/v) u_c}{\rho_c^2} \right)^{1/4} \quad (2.16)$$

Where

k_l = mass transfer coefficient (m/s).

Sc = Schmidt number (dimension less).

P/v = power input per unit volume estimated from fig (2.8).

μ_c = viscosity of continuous phase (poise).

ρ_c = density of continuous phase (Kg/m³).

From experimental data for corrosion rate, mass transfer coefficient was calculated.

$$N_A = k C_b \quad (3.13)$$

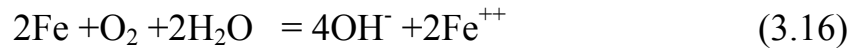
Where :

N_A = mass flux (mol O₂/m² s).

k = mass transfer coefficient (m/s).

c_b = concentration (mol O₂/ m³).

Converting corrosion rate to mass flux.



$$N_A = \left(\frac{C.R_{gmd}}{mwt_{Fe} / 2} \right) \left(\frac{1}{3600 * 24} \right) \quad (3.17)$$

Then calculate mass transfer coefficient from equation (3-13). Tables (3-5,6) show the calculations. Concentration of oxygen calculated from solubility of oxygen in water per one second.

Table (3-5) Mass transfer coefficient calculated from experimental corrosion rate of iron in a mixture of kerosene and water at 25 °C.

RPM ⁽³⁶⁾	% ⁽³⁶⁾	C.R _{Exp.} gmd ⁽³⁶⁾	C.R x 10 ⁶ molO ₂ /m ² .s	Mol O ₂ /m ³	k x10 ⁵ _{Exp.} (m/s)
270	0.05	41.029	4.255	0.258	1.649
320	0.05	44.991	4.666	0.258	1.809
450	0.05	48.658	5.046	0.258	1.956
270	0.15	50.314	5.218	0.258	2.022
320	0.15	56.729	5.883	0.258	2.280
450	0.15	75.031	7.781	0.258	3.016
270	0.3	51.723	5.364	0.258	2.079
320	0.3	67.515	7.002	0.258	2.714

Table (3-6) Mass transfer coefficient calculated from experimental corrosion rate of iron in a mixture of kerosene and water at 40 °C.

RPM ⁽³⁷⁾	% ⁽³⁷⁾	C.R _{Exp.} gmd ⁽³⁷⁾	C.R x 10 ⁶ molO ₂ /m ² .s	Mol O ₂ /m ³	k x10 ⁶ _{Exp.} (m/s)
600	0.01	9.306	0.9651	0.2	4.83
800	0.01	14.204	1.473	0.2	7.37
1000	0.01	19.102	1.981	0.2	9.91
1200	0.01	21.55	2.235	0.2	11.18
1400	0.01	29.87	3.098	0.2	15.49
600	0.05	16.65	1.726	0.2	8.63
800	0.05	20.08	2.0825	0.2	10.41
1000	0.05	24	2.489	0.2	12.45
1200	0.05	25.9	2.686	0.2	13.43
1400	0.05	32.816	3.403	0.2	17.02
600	0.1	66.613	6.908	0.2	34.54
800	0.1	73.47	7.62	0.2	38.10
1000	0.1	79.48	8.243	0.2	41.22
1200	0.1	84.61	8.775	0.2	43.88
1400	0.1	95.63	9.9178	0.2	49.59
600	0.2	74.26	7.702	0.2	38.51
800	0.2	77.16	8	0.2	40.00
1000	0.2	86.93	9.016	0.2	45.08
1200	0.2	93.76	9.724	0.2	48.62
1400	0.2	105.61	10.95	0.2	54.75

Table (3-7) Mass transfer coefficient calculated from equation (2-16) at 25°C.

$\phi^{(36)}$	Re	NP from fig.(3.5)	P(J/s)	P/V	Sc	$k_L \times 10^5$ (m/s)
0.05	11879(270)	6	1.41	0.39	1278	7.00
0.05	14079(320)	5.8	2.26	0.63	1278	7.88
0.05	19799(450)	5.8	6.29	1.75	1278	10.17
0.15	13074(270)	5.8	1.41	0.39	1244	7.13
0.15	15495(320)	5.8	2.26	0.63	1244	8.02
0.15	21790(450)	5.8	6.29	1.75	1244	10.36
0.3	15235(270)	5.8	1.36	0.38	1195	7.26
0.3	18057(320)	5.8	2.26	0.63	1195	8.24

Table (3-8) Mass transfer coefficient calculated from equation (2-16) at 40°C.

$\varphi^{(37)}$	Re	NP from fig.(3-5)	P(J/s)	P/V	Sc	$k_L \times 10^5$ (m/s)
0.01	23824(600)	5.8	14.75	1.20	778.66	1.24
0.01	31765(800)	5.8	34.96	2.84	778.66	1.54
0.01	39707(1000)	5.8	68.29	5.55	778.66	1.82
0.01	47648(1200)	5.8	118.01	9.59	778.66	2.08
0.01	55589(1400)	5.8	187.39	15.23	778.66	2.34
0.05	24957(600)	5.8	14.75	1.20	743.41	1.28
0.05	33276(800)	5.8	34.96	2.84	743.41	1.59
0.05	41596(1000)	5.8	68.29	5.55	743.41	1.88
0.05	49915(1200)	5.8	118.01	9.59	743.41	2.16
0.05	58234(1400)	5.8	187.39	15.23	743.41	2.42
0.1	26051(600)	5.8	14.75	1.20	712.09	1.32
0.1	34735(800)	5.8	34.96	2.84	712.09	1.64
0.1	43419(1000)	5.8	68.29	5.55	712.09	1.93
0.1	52102(1200)	5.8	118.01	9.59	712.09	2.22
0.1	60786(1400)	5.8	187.39	15.23	712.09	2.49
0.2	28910(600)	5.8	14.75	1.20	641.67	1.41
0.2	38547(800)	5.8	34.96	2.84	641.67	1.75
0.2	48184(1000)	5.8	68.29	5.55	641.67	2.07
0.2	57820(1200)	5.8	118.01	9.59	641.67	2.38
0.2	67457(1400)	5.8	187.39	15.23	641.67	2.67

Since corrosion rate is mass transfer controlled in nearly neutral aqueous solution, the corrosion rates have calculated from the value of mass transfer coefficients equation (3-13) which has been calculated from equation (3-12). These calculation illustrated in tables (3-9,10).

Table (3-9) Corrosion rate calculated from equation (2-16) at 25°C.

$\%^{(36)}$	$k_L \times 10^6$ (m/s)	mol O ₂ /m ³	C.R cal.x 10 ⁶ Mole O ₂ /m ² .s
0.05	7.00	0.258	1.81
0.05	7.88	0.258	2.03
0.05	10.17	0.258	2.62
0.15	7.13	0.258	1.84
0.15	8.02	0.258	2.07
0.15	10.36	0.258	2.67
0.3	7.26	0.258	1.87
0.3	8.24	0.258	2.13

Table (3-10) Corrosion rate calculated from equation (2-16) at 40°C.

$\%^{(37)}$	$k_L \times 10^5$ (m/s)	mol O ₂ /m ³	C.R _{cal.} x 10 ⁶ Mole O ₂ /m ² .s
0.01	1.24	0.2	2.48
0.01	1.54	0.2	3.08
0.01	1.82	0.2	3.64
0.01	2.08	0.2	4.16
0.01	2.34	0.2	4.68
0.05	1.28	0.2	2.56
0.05	1.59	0.2	3.18
0.05	1.88	0.2	3.76
0.05	2.16	0.2	4.32
0.05	2.42	0.2	4.84
0.1	1.32	0.2	2.64
0.1	1.64	0.2	3.28
0.1	1.93	0.2	3.86
0.1	2.22	0.2	4.44
0.1	2.49	0.2	4.98
0.2	1.41	0.2	2.82
0.2	1.75	0.2	3.5
0.2	2.07	0.2	4.14
0.2	2.38	0.2	4.76
0.2	2.67	0.2	5.34

3-7 Two Ways Analysis (ANOVA)

At rpm =450 and water volume percent 30% there is missing experimental data point calculated from the following equation ⁽³⁸⁾.

$$X = \frac{rR + cC - S}{(r - 1)(c - 1)} \quad \dots\dots\dots(3-13)$$

Where

X= missing data.

r = number of rows.

c = number of columns.

R = total of rows with missing data point.

C = total of columns with missing data point.

S = total of all known data.

Table (3-11) Data of corrosion rate (gmd) at 25⁰C

	270		320		450		
5%	403.94		484.65		446.34		
	399.48	410.29	423.04	449.92	557.49	486.58	448.93
	427.45		442.06		455.92		
15%	487.51		558.7		786.02		
	522.54	503.14	579.73	567.29	755.95	750.31	606.91
	499.36		563.43		708.95		
30%	508.33		668.02		720.66*		
	478.51	517.23	702.89	675.14	766.22*	731.98	641.45
	564.84		654.54		709.05*		
	476.89		564.12		656.29		565.7644

* The missing points, Eq.(3-13).

- SS_{within} and df_{within}

$$SS_{\text{within}} = \sum_{i=1}^3 \sum_{j=1}^3 \sum_{k=1}^3 (Y_{ijk} - Y_{ij})^2$$

$$\begin{aligned}
&= (403.94 - 410.29)^2 + (399.48 - 410.29)^2 + (427.45 - 410.29)^2 + \\
&\quad (484.65 - 449.92)^2 + (423.04 - 449.92)^2 + (442.06 - 449.92)^2 + \\
&\quad (446.34 - 486.58)^2 + (557.49 - 486.58)^2 + (455.92 - 486.58)^2 + \\
&\quad (487.34 - 503.14)^2 + (522.54 - 503.14)^2 + (499.34 - 503.14)^2 + \\
&\quad (558.7 - 567.29)^2 + (579.73 - 567.29)^2 + (563.43 - 567.29)^2 + \\
&\quad (786.02 - 750.31)^2 + (755.95 - 750.31)^2 + (708.95 - 750.31)^2 + \\
&\quad (508.33 - 517.23)^2 + (478.51 - 517.23)^2 + (564.84 - 513.23)^2 + \\
&\quad (668.02 - 675.14)^2 + (702.89 - 675.14)^2 + (654.54 - 675.14)^2 + \\
&\quad (720.66 - 731.98)^2 + (766.22 - 731.98)^2 + (709.05 - 731.98)^2 \\
&= 21,238.87
\end{aligned}$$

$$\begin{aligned}
df_{\text{within}} &= (r-1) ab \\
&= (3-1) \times 3 \times 3 = 18
\end{aligned}$$

$$MS_{\text{within}} = 21,238.87/18 = 1,179.94$$

- SS_{Ψ} and df_{Ψ}

$$\begin{aligned}
SS_{\Psi} &= r.b \sum_{i=1}^3 (Y_i - Y_{..})^2 \\
&= 9 [(448.93 - 565.78)^2 + (606.91 - 565.78)^2 + (632.94 - 565.78)^2] \\
&= 178,701.51
\end{aligned}$$

$$\begin{aligned}
df_{\Psi} &= a-1 \\
&= 3-1=2
\end{aligned}$$

$$MS_{\Psi} = 178701.51/2 = 89,350.76$$

- SS_{rpm} and df_{rpm}

$$\begin{aligned}
SS_{\text{rpm}} &= r.a \sum_{j=1}^3 (Y_j - Y_{..})^2 \\
&= 9 [(476.89 - 565.76)^2 + (564.12 - 565.76)^2 + (656.29 - 565.76)^2] \\
&= 144,866.23
\end{aligned}$$

$$\begin{aligned}
df_{\text{rpm}} &= b-1 \\
&= 3-1=2
\end{aligned}$$

$$MS_{rpm} = 144,866.23/2 = 72,433.23$$

- $SS_{interaction}$ and $df_{interaction}$

$$\begin{aligned} SS_{interaction} &= r \sum_{i=1}^3 \sum_{j=1}^3 (Y_{ijk} - Y_{...} - Y_i + Y_{...})^2 \\ &= 3[(410.29-448.93-476.89+565.76)^2 + (449.92-448.93-564.12+565.76)^2 + (486.58-448.93-656.29+565.76)^2 + \\ &\quad (503.14-606.91-564.12+565.76)^2 + (567.29-564.12-606.91+565.76)^2 + (750.31-606.91-656.29+565.76)^2 + \\ &\quad (517.23-476.89-641.45+565.76)^2 + (675.14-641.45-564.12+565.76)^2 + (731.98-641.45-656.29+565.76)^2 + \\ &\quad (410.29-476.89-448.93+565.76)^2 + (449.92-564.12-446.93+565.76)^2 + (486.58-656.29-448.93+565.76)^2 + \\ &\quad (503.14-476.89-606.91+565.76)^2 + (567.29-606.91-564.12+565.76)^2 + (750.31-656.29-606.91+565.76)^2 + \\ &\quad (514.23-641.45-476.89+565.76)^2 + (675.14-564.12-641.45+565.76)^2 + (731.98-656.29-641.45+565.76)^2] \\ &= 104,328.51 \end{aligned}$$

$$\begin{aligned} df_{interaction} &= (a-1)(b-1) \\ &= (3-1)(3-1) = 4 \end{aligned}$$

$$MS_{interaction} = 104,328.51/4 = 26,082.13$$

Table (3-12) Analysis of variance for corrosion rate at 25⁰C

Source	Df	SS	MS	F	F _{0.05}	F _{0.01}
Re	2	144866.23	72433.23	61.39	3.55	6.01
Ψ	2	178701.51	89350.76	75.73	3.55	6.01
Re XΨ	4	104328.51	26082.13	22.10	2.93	4.58
Within	18	21238.87	1179.94			
Total	26	449135.1				

Table (3-13) Data of Sauter mean diameter at 25⁰C

	270	320	450	Total	Mean
5%	1.40E-05	1.14E-05	7.56E-06	3.31E-05	1.10E-05
15%	1.99E-05	1.62E-05	1.08E-05	4.69E-05	1.56E-05
30%	2.88E-05	2.35E-05	2.00E-05*	7.23E-05	2.41E-05
Total	6.27E-05	5.11E-05	3.83E-05	1.52E-04	5.07E-05
Mean	2.09E-05	1.70E-05	1.28E-05	5.07E-05	1.69E-05

* missing point, eq.(3-13)

$$C = T^2/r.c$$

$$= (1.521 \times 10^{-4})^2 / 9 = 2.57 \times 10^{-9}$$

$$SSR = \sum T_i^2 / c - C$$

$$= ((3.31 \times 10^{-5})^2 + (4.69 \times 10^{-5})^2 + (7.228 \times 10^{-5})^2 / 3) - 2.57 \times 10^{-9}$$

$$= 2.6495 \times 10^{-10}$$

$$SSC = \sum T_j^2 / r - C$$

$$= ((6.27 \times 10^{-5})^2 + (5.11 \times 10^{-5})^2 + (3.83 \times 10^{-5})^2 / 3) - 2.57 \times 10^{-9}$$

$$= 9.897 \times 10^{-10}$$

$$SST = \sum_{i=1}^c \sum_{j=1}^r x_{ij}^2 - C$$

$$= [(1.4 \times 10^{-5})^2 + (1.99 \times 10^{-5})^2 + (2.88 \times 10^{-5})^2 + (1.14 \times 10^{-5})^2 +$$

$$(1.62 \times 10^{-5})^2 + (2.35 \times 10^{-5})^2 + (0.756 \times 10^{-5})^2 + (1.08 \times 10^{-5})^2$$

$$+ (1.998 \times 10^{-5})^2] - 2.57 \times 10^{-9}$$

$$= 3.672 \times 10^{-10}$$

$$SSE = SST - SSR - SSC$$

$$= 3.672 \times 10^{-10} - 2.649 \times 10^{-10} - 9.897 \times 10^{-11}$$

$$= 3.328 \times 10^{-12}$$

$$MSC = SSC/c-1 = 9.897 \times 10^{-10} / 2 = 4.95 \times 10^{-11}$$

$$MSR = SSR/r-1 = 2.649 \times 10^{-10} / 2 = 1.326 \times 10^{-11}$$

$$MSE = SSE/(r-1)(c-1) = 3.328 \times 10^{-12}/4 = 8.32 \times 10^{-13}$$

$$F_R = MSR/MSE = 1.32 \times 10^{-11}/8.32 \times 10^{-13} = 159.38$$

$$F_C = MSC/MSE = 4.95 \times 10^{-11}/8.32 \times 10^{-13} = 59.38$$

Table (3-14) Analysis of variance for Sauter mean diameter at 25°C.

Source	SS	Df	MS	F	F _{0.05}	F _{0.01}
Column	9.8976E-11	2	4.94E-11	59.38	6.94	18
Rows	2.6495E-10	2	1.326E-11	159.38	6.94	18
Error	3.328E-12	4	8.321E-13			
Total	3.674E-10	8				

Table (3-15) Total number of droplets per unit volume at 25°C.

	270	320	450	Total	Mean
5%	1.19E+12	2.20E+12	7.50E+12	1.09E+13	3.63E+12
15%	1.24E+12	2.28E+12	7.77E+12	1.13E+13	3.76E+12
30%	8.14E+11	1.77E+10	7.08E+12*	7.92E+12	2.64E+12
Total	3.25E+12	4.49E+12	2.23E+13	3.01E+13	1.00E+13
Mean	1.08E+12	1.50E+12	7.45E+12	1.00E+13	3.34E+12

* missing point, eq.(3-13)

Table (3-16) Analysis of variance for total number of droplets per unit volume at 25⁰C.

Source	SS	Df	MS	F	F _{0.05}	F _{0.01}
Column	7.6146E+25	2	3.8073E+25	110.81	6.94	18
Rows	2.2715E+24	2	1.1357E+24	3.31	6.94	18
Error	1.3744E+24	4	3.436E+23			
Total	7.9792E+25	8				

Table (3-17) Data of corrosion rate at 40⁰C.

	600	800	1000	1200	1400	Total	Mean
1%	9.306	14.204	19.102	21.55	29.87	94.03	23.51
5%	16.65	20.08	24.00	25.90	32.826	119.45	29.86
10%	66.613	73.47	79.48	84.61	95.63	399.80	99.95
20%	74.26	77.16	86.93	93.76	105.61	437.72	109.43
Total	166.83	184.91	209.51	225.82	263.93	1051.00	262.75
Mean	41.71	46.23	52.38	56.46	65.98	262.75	65.69

Table (3-18) Analysis of variance for corrosion rate at 40⁰C.

Source	SS	Df	MS	F	F _{0.05}	F _{0.01}
Column	1413.1	4	353.28	36.38	3.26	5.41
Rows	19679.4	3	6559.8	675.47	3.49	5.95
Error	116.5	12	9.71			
Total	21209					

Table (3-19) Data of Sauter mean diameter at 40⁰C.

	600	800	1000	1200	1400	Total	Mean
1%	4.25E-06	3.00E-06	2.30E-06	1.85E-06	1.54E-06	1.29E-05	3.24E-06
5%	5.12E-06	3.63E-06	2.77E-06	2.23E-06	1.85E-06	1.56E-05	3.90E-06
10%	6.21E-06	4.40E-06	3.36E-06	2.70E-06	2.25E-06	1.89E-05	4.73E-06
20%	8.39E-06	5.94E-06	4.54E-06	3.65E-06	3.03E-06	2.56E-05	6.39E-06
Total	2.40E-05	1.70E-05	1.30E-05	1.04E-05	8.67E-06	7.30E-05	1.83E-05
Mean	5.99E-06	4.24E-06	3.24E-06	2.61E-06	2.17E-06	1.83E-05	4.56E-06

Table (3-20) Analysis of variance for Sauter mean diameter at 40⁰C.

Source	SS	Df	MS	F	F _{0.05.}	F _{0.01.}
Column	37.1561	4	9.29	44.72	3.26	5.41
Rows	17.7915	3	5.9305	28.55	3.49	5.95
Error	2.4926	12	0.20771			
Total	57.4401	19				

Table (3-21) Data of total number of droplets per unit volume at 40°C.

	600	800	1000	1200	1400	Total	Mean
1%	2.47E+11	6.95E+11	1.55E+12	2.99E+12	5.21E+12	1.07E+13	2.68E+12
5%	7.06E+11	1.99E+12	4.44E+12	8.56E+12	1.49E+13	3.06E+13	7.65E+12
10%	7.92E+11	2.23E+12	4.98E+12	9.60E+12	1.67E+13	3.43E+13	8.58E+12
20%	6.42E+11	1.81E+12	4.04E+12	7.79E+12	1.36E+13	2.79E+13	6.96E+12
Total	2.39E+12	6.72E+12	1.50E+13	2.89E+13	5.04E+13	1.03E+14	2.59E+13
Mean	5.97E+11	1.68E+12	3.75E+12	7.23E+12	1.26E+13	2.59E+13	6.47E+12

Table (3-22) Analysis of variance for total number of droplets per unit volume at 40°C.

Source	SS	Df	MS	F	F _{0.05}	F _{0.01}
Column	3.784E+26	4	9.45E+25	24.52	3.2	5.41
Rows	6.5571E+25	3	2.186E+25	5.67	3.49	5.95
Error	4.6292E+25	12	3.86E+24			
Total	4.9027E+26	19				

CHAPTER FOUR

DISCUSSION

4.1 Introduction

Corrosion process is a resultant of several important factors. Therefore discussions of the process necessitate a considerable attention need to be given to each factor, in respect of its effect and behavior. Consideration of these factors shows that complexities exist which may modify the observable corrosion effect ⁽³⁹⁾. Despite the importance of other factors water (moisture) remains the key factor in corrosion process. The effects of the most important factors together in single phase and two phase flow are discussed in this chapter.

4.2 Single phase (100% Vol. aqueous solution).

Natural water is relatively non -corrosive in absence of oxygen, the corrosion rate of steel is approximately proportional to the concentration of oxygen in water up to about saturation by air at one atmosphere. Salts dissolved in water have a marked influence on the corrosivity of water. Generally, the corrosivity of water containing dissolved salts increased with increasing salt concentration until a maximum is reached, and then corrosivity decreased. This may be attributed to increased electconductivity because of the increased salt content, until the salt concentration is great enough to cause an appreciable decrease in the oxygen solubility.

The rate of corrosion increases many times under the influence of agitation which enhances the amount of oxygen transfer to the metal specimens, i.e, increased agitation leads to increased limiting current density.

4.3 Two phase (water/oil)

The understanding of mixing operations in stirred tanks cannot be achieved without obtaining a better picture of the flow phenomena in them.

In turbulent dispersion drops show complicated motion, because they are acted on by turbulence components as well as mean flow currents of the surrounding liquid. Any formulation of the effect or knowledge of the turbulent behavior of liquid flow is considerably important for illustration of corrosion under two phase flow⁽⁴⁰⁾.

The first step in the study of fluid and drops motion in turbulent dispersion may be fundamental and detailed knowledge of the turbulence characteristics of the liquid flow is also important. Turbulent flow characteristics indicated many inherent experimental difficulties, especially when applied to heterogeneous systems containing drops of the dispersed phase. Consequently, the experimental studies of turbulence in liquid system are still in the early stage of the development, or, at least, they are slowly developing⁽⁴¹⁾.

In the light of the above points it can be seen how much the hydrodynamics of agitation system is complex and become even more difficult to understand in the case of dispersion system of immiscible liquids.

4.3.1 Effect of Reynolds number and Weber number:

If a certain mass of liquid is placed in a turbulent stream of an immiscible liquid, the liquid will break up under the influence of turbulence eddies. It is related to the fact that velocity in turbulent liquid stream varies from one point to another. Some attempts were made theoretically and experimentally to evaluate the effective relative velocity in turbulent dispersions.

However, some limitations were noticed. The droplets in turbulent dispersion respond to fluid motion depending on their diameter and density

difference. If droplets are large compared to the macro-scale of turbulence, they will at most follow the bulk flow current ⁽⁴²⁾.

Corrosion rates even when controlled by diffusion are not always simply related to mass transfer, especially for specimens with non-uniform flow conditions.

The influence of hydrodynamics on corrosion is a rather complicated process as corrosion is controlled by mass transport through a damped turbulent boundary layer followed by transport through a porous corrosion product layer. In two phase systems fluid hydrodynamics are even more complicated. In addition to this corrosion is generally enhanced as oxygen solubility in kerosene is many times higher than that of the aqueous phase ⁽⁴³⁾.

The influence of increased Re ., i.e., increased turbulence, is to increase the number of dispersed aqueous phase droplets which are found to be a function of We . Agitator Reynolds number Re describes the type of flow near the impeller. Increasing Re or We would lead to greater number of droplets and thus lead to more intimate contact between the dispersed phase droplets and the metal specimens. The following figures show the relation between the corrosion rate (calculated and experimental) according to tables ((3-5), (3-6) and (3-9),(3-10))at (25 and 40°C) and total number of droplet per unit volume with Reynolds number and Weber number.

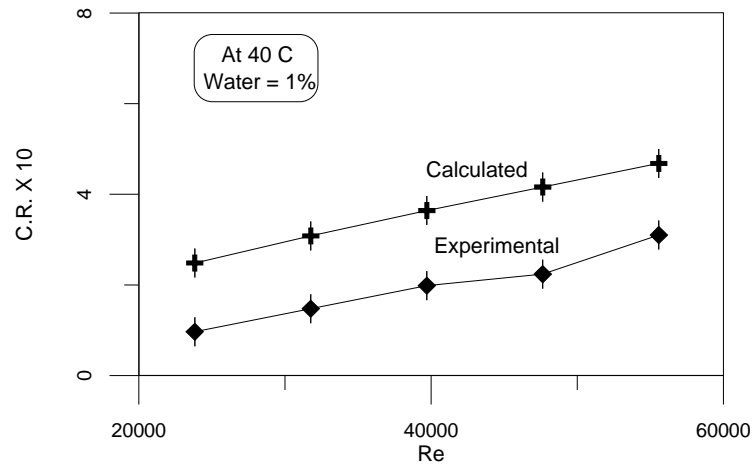


Figure (4-1) Relation between corrosion rate (gmd) (experimental and calculated) vs. Reynolds number at 40 °C ,%water=0.01.

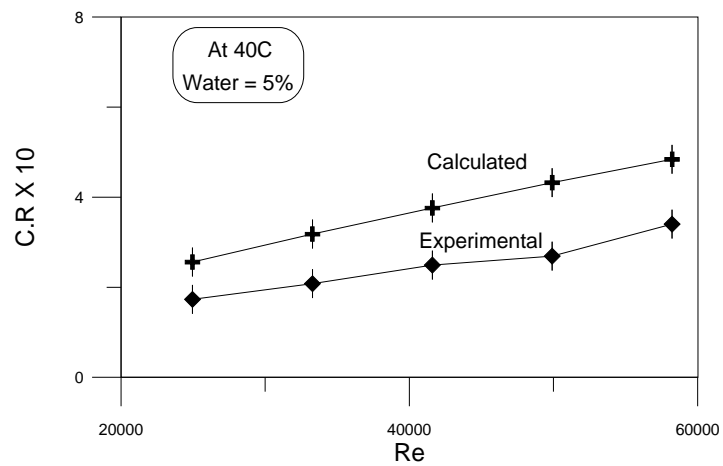


Figure (4-2) Relation between corrosion rate(gmd) (experimental and calculated) vs. Reynolds number at 40 °C ,%water=0.05.

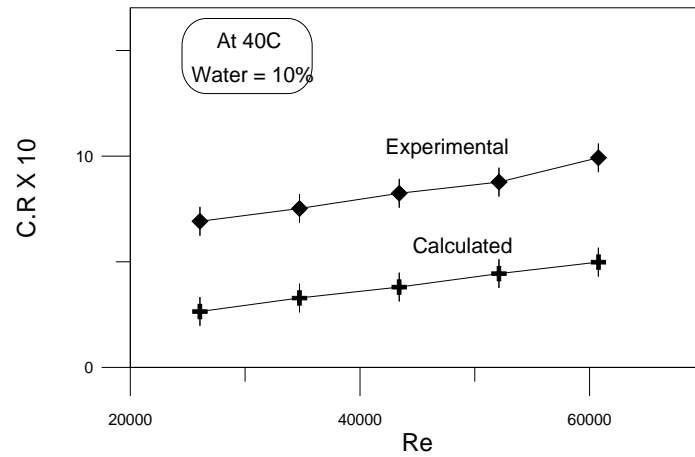


Figure (4-3) Relation between corrosion rate(gmd) (experimental and calculated) vs. Reynolds number at 40 °C ,%water=0.1.

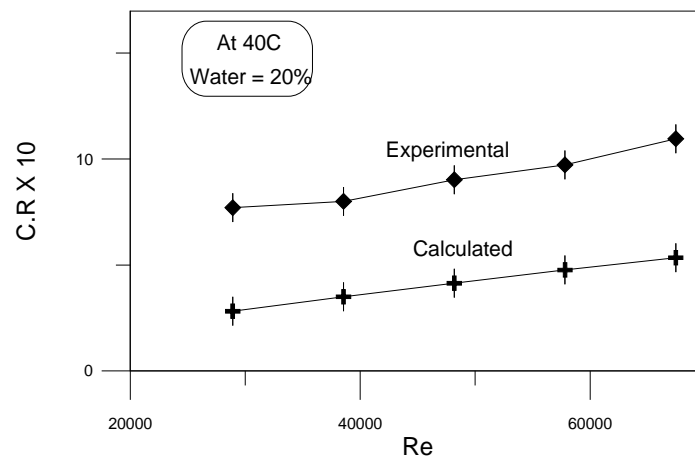


Figure (4-4) Relation between corrosion rate(gmd) (experimental and calculated) vs. Reynolds number at 40 °C ,%water=0.2.

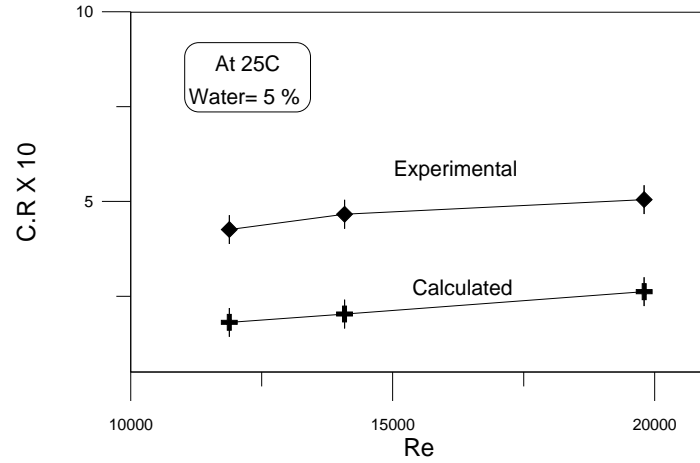


Figure (4-5) Relation between corrosion rate (gmd) (experimental and calculated) vs. Reynolds number at 25 °C ,%water=0.05.

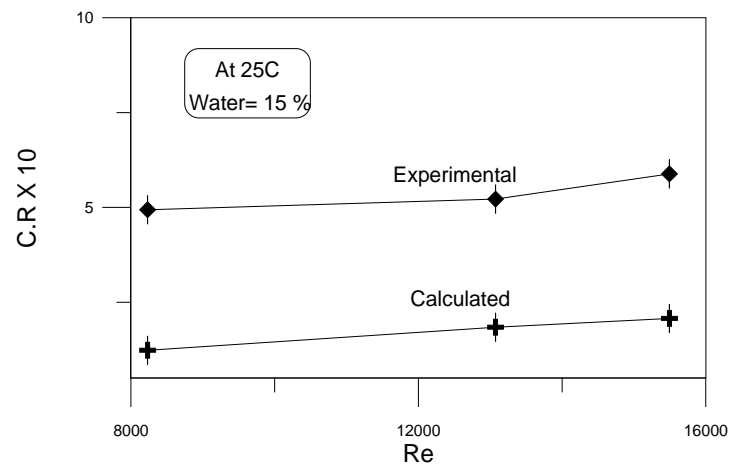


Figure (4-6) Relation between corrosion rate (gmd) (experimental and calculated) vs. Reynolds number at 25 °C ,%water=0.15.

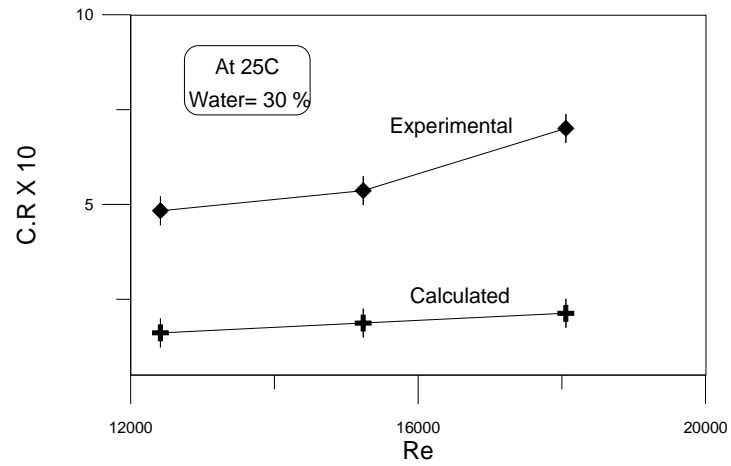


Figure (4-7) Relation between corrosion rate(gmd) (experimental and calculated) vs. Reynolds number at 25 °C ,%water=0.3.

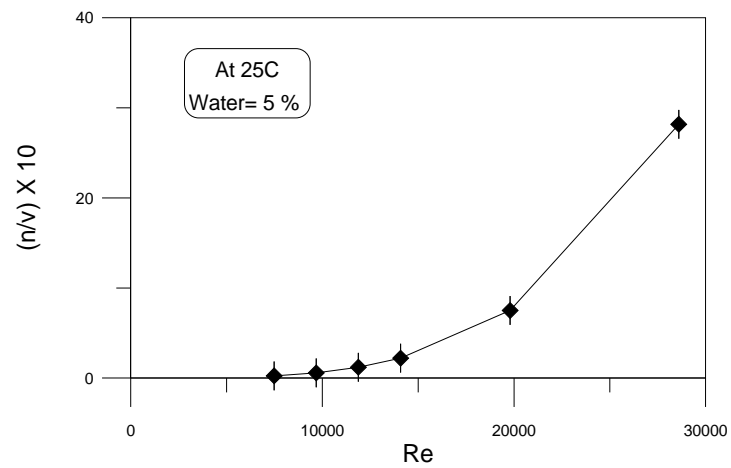


Figure (4-8) Relation between Reynolds number and total number of droplets per unit volume at 25 °C ,%water=0.05.

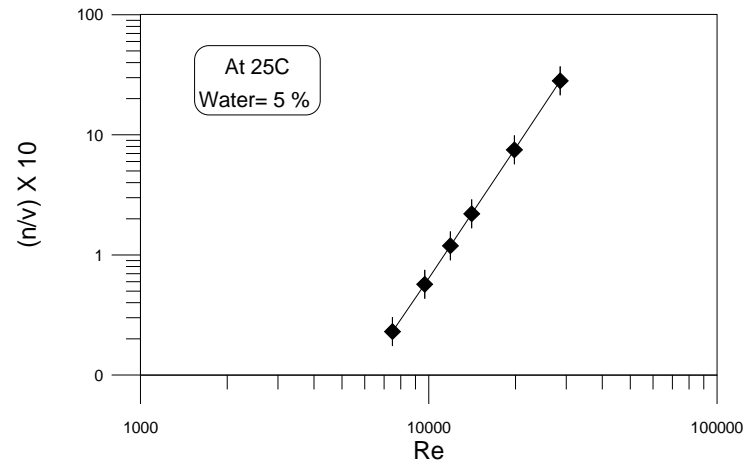


Figure (4-9) Relation between log total number of droplets per unit volume and log Reynolds number at 25 °C ,%water=0.05.

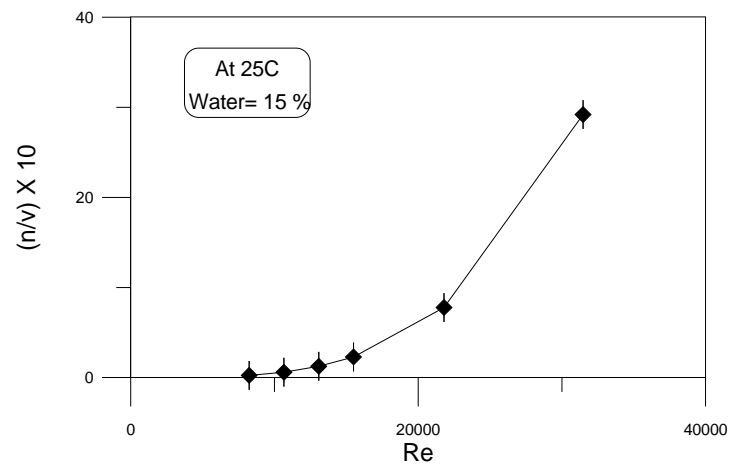


Figure (4-10) Relation between Reynolds number and total number of droplets per unit volume at 25 °C, %water=0.15.

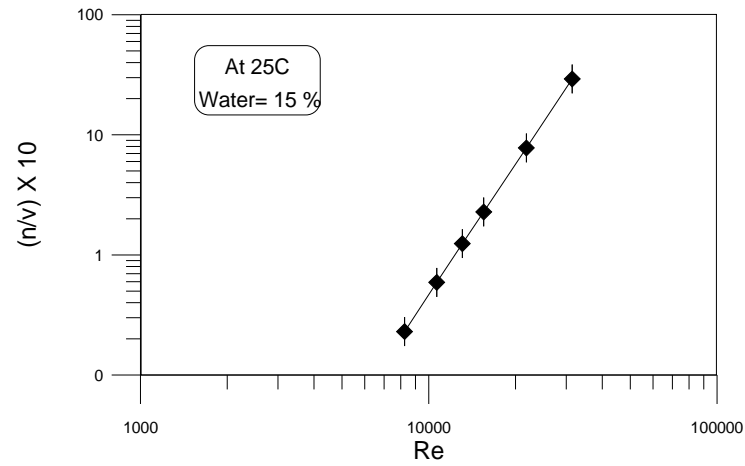


Figure (4-11) Relation between log total number of droplets per unit volume and log Reynolds number at 25 °C, %water=0.15.

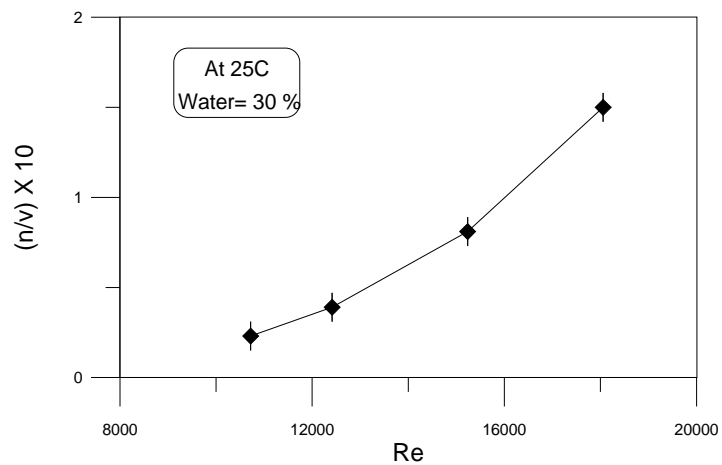


Figure (4-12) Relation between Reynolds number and total number of droplets per unit volume at 25 °C, %water=0.3.

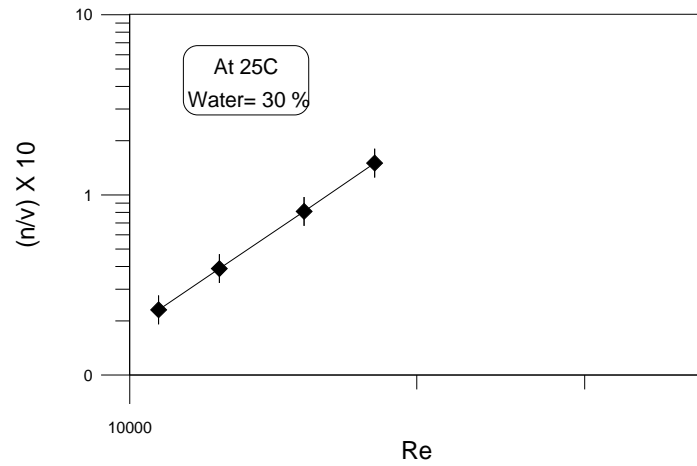


Figure (4-13) Relation between log total number of droplets per unit volume and log Reynolds number at 25 °C, %water=0.3.

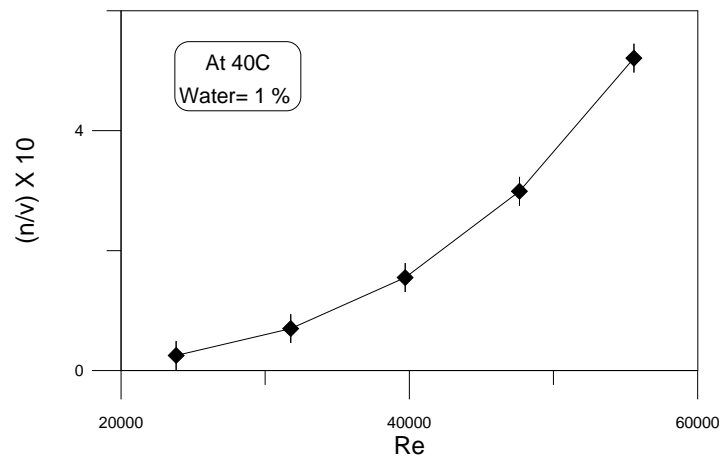


Figure (4-14) Relation between Reynolds number and total number of droplets per unit volume at 40 °C ,%water=0.01.

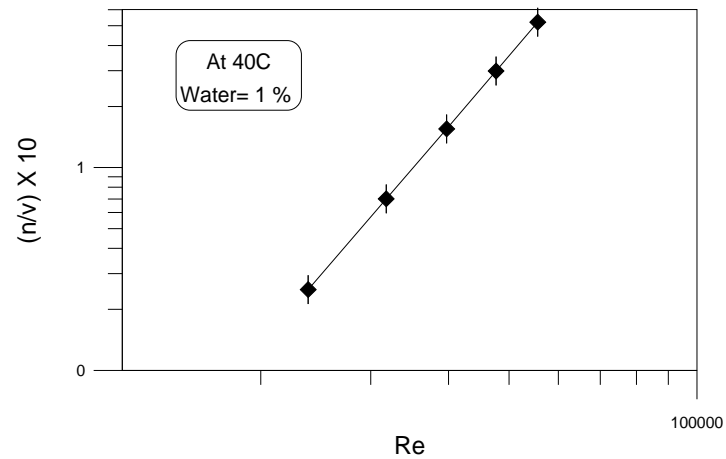


Figure (4-15) Relation between log total number of droplets per unit volume and log Reynolds number at 40 °C ,%water=0.01.

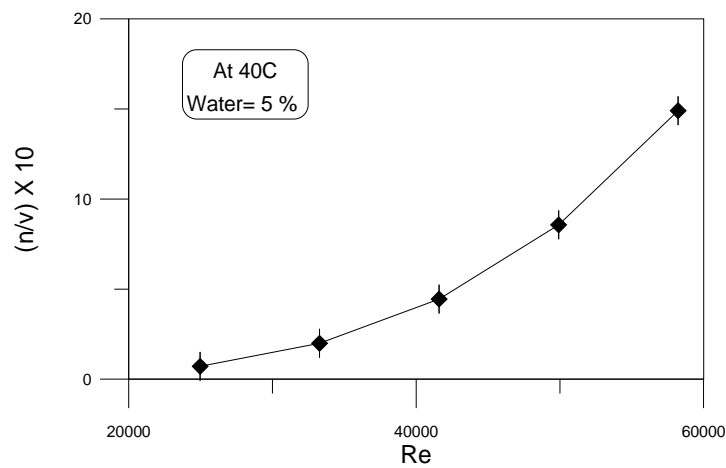


Figure (4-16) Relation between Reynolds number and total number of droplets per unit volume at 40 °C ,%water=0.05.

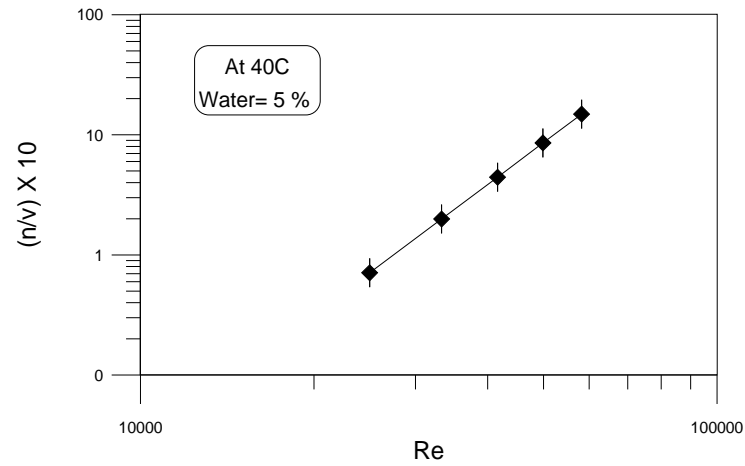


Figure (4-17) Relation between log total number of droplets per unit volume and log Reynolds number at 40 °C ,%water=0.05.

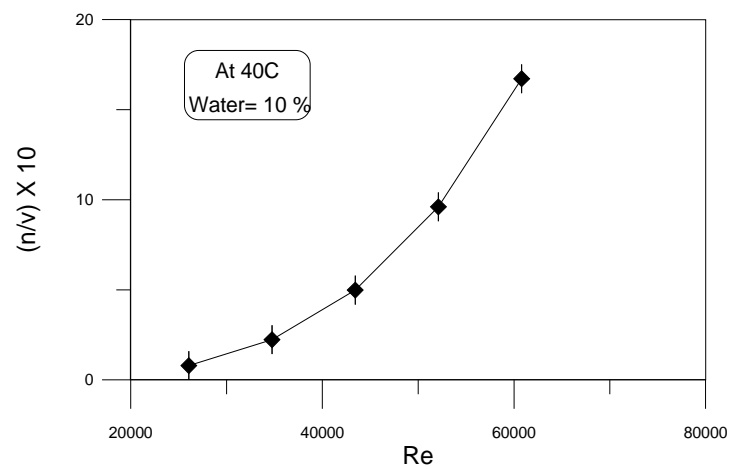


Figure (4-18) Relation between Reynolds number and total number of droplets per unit volume at 40 °C ,%water=0.1.

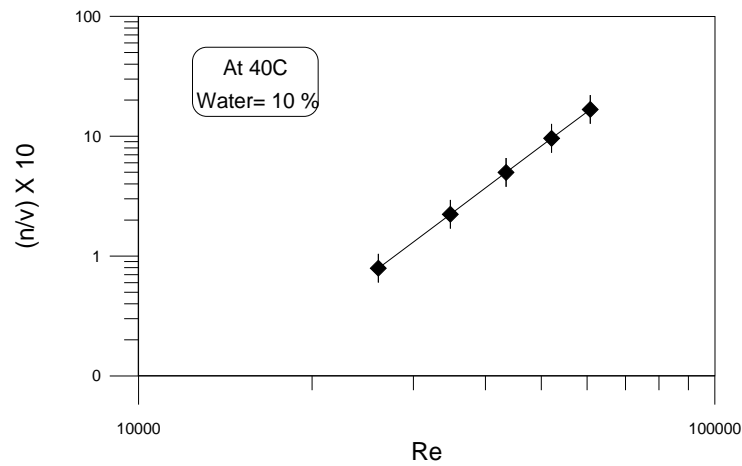


Figure (4-19) Relation between log total number of droplets per unit volume and log Reynolds number at 40 °C ,%water=0.1.

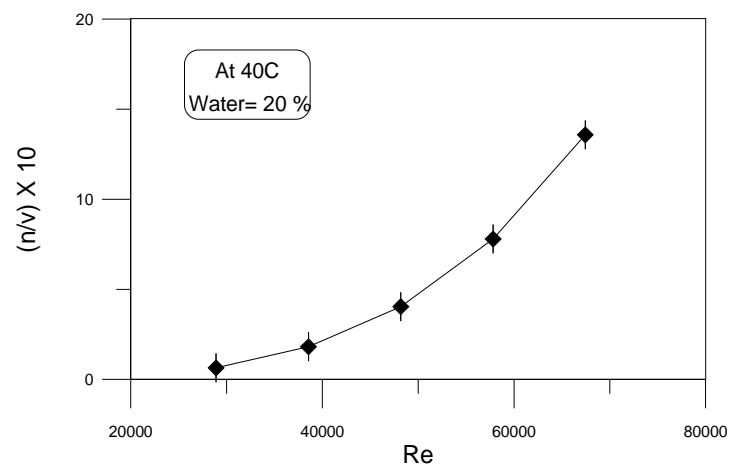


Figure (4-20) Relation between Reynolds number and total number of droplets per unit volume at 40 °C ,%water=0.2.

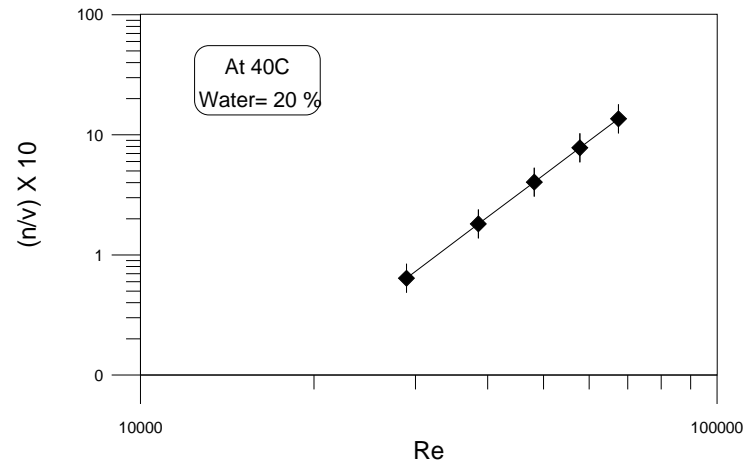


Figure (4-21) Relation between log total number of droplets per unit volume and log Reynolds number at 40 °C ,%water=0.2.

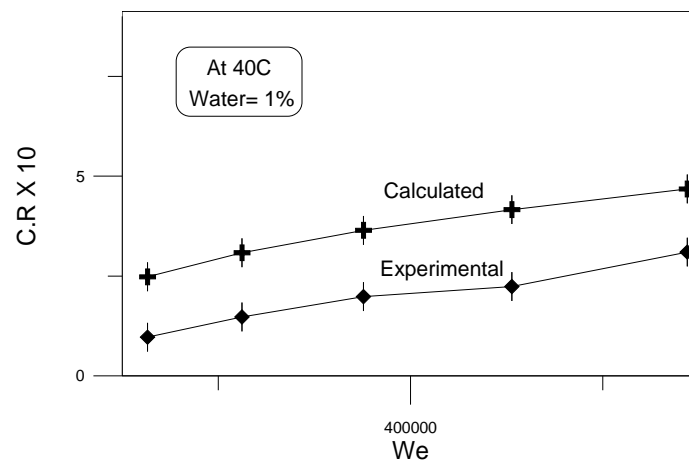


Figure (4-22) Relation between corrosion rate (experimental and calculated) vs. Weber number at 40 °C ,%water=0.01.

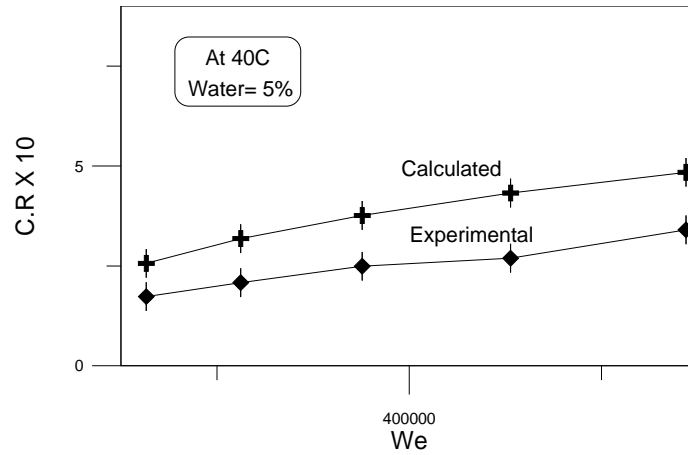


Figure (4-23) Relation between corrosion rate(gmd) (experimental and calculated) vs. Weber number at 40 °C ,%water=0.05.

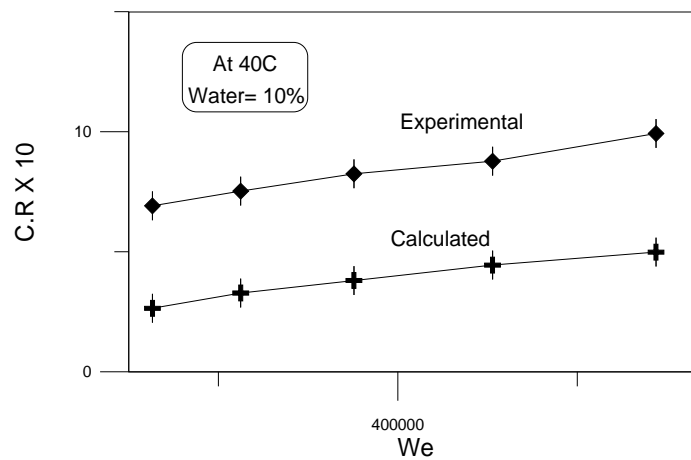


Figure (4-24) Relation between corrosion rate(gmd) (experimental and calculated) vs. Weber number at 40 °C, %water=0.1.

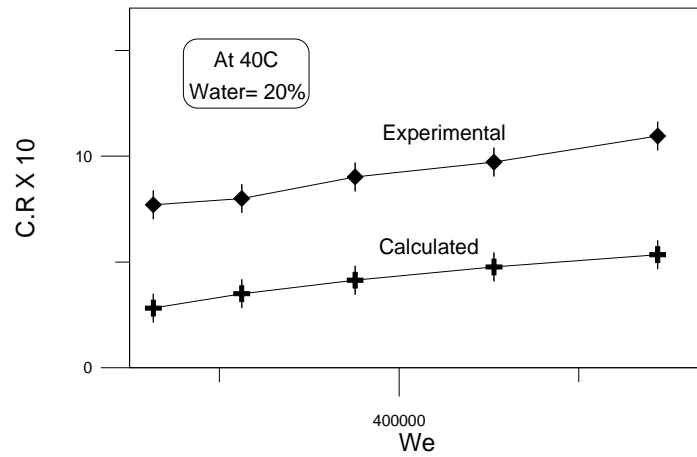


Figure (4-25) Relation between corrosion rate(gmd) (experimental and calculated) vs. Weber number at 40 °C, %water=0.2.

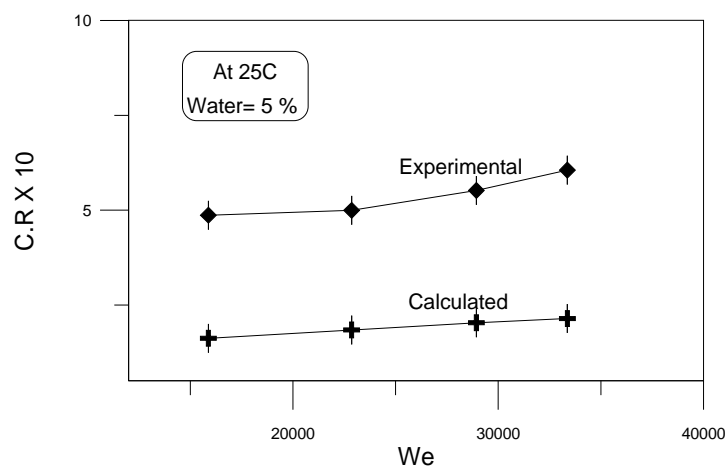


Figure (4-26) Relation between corrosion rate(gmd) (experimental and calculated) vs. Weber number at 25 °C, %water=0.05.

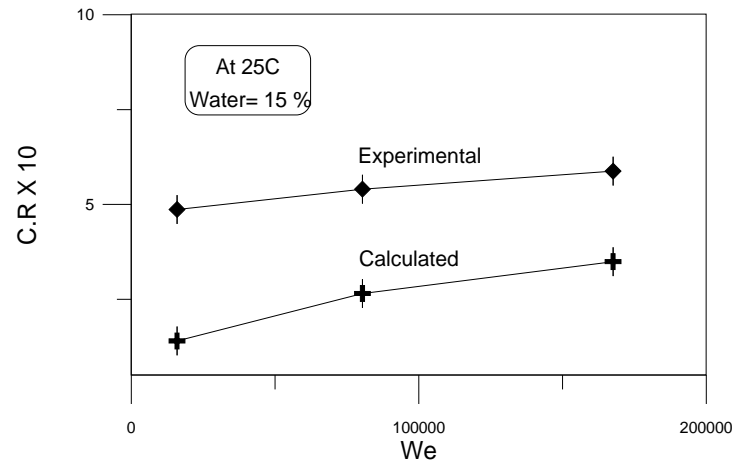


Figure (4-27) Relation between corrosion rate(gmd) (experimental and calculated) vs. Weber number at 25 ⁰C, %water=0.15.

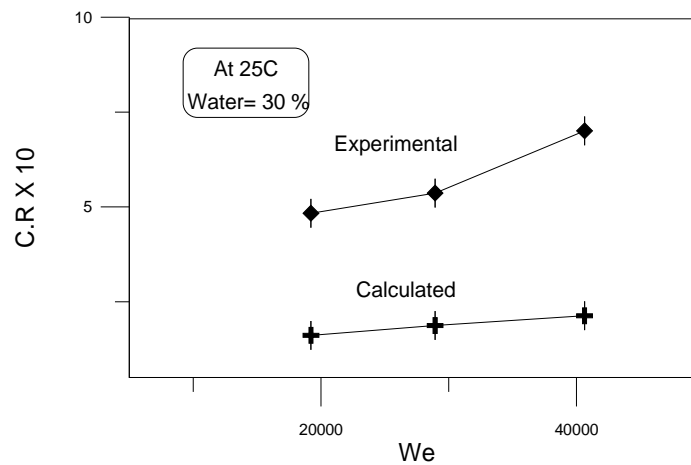


Figure (4-28) Relation between corrosion rate(gmd) (experimental and calculated) vs. Weber number at 25 ⁰C, %water=0.3.

It is clear from Tables (3-1), (3-2) that specific surface area (a) and number of droplets per unit volume (n/v) increase as rpm or Re increase at 25 and 40 °C.

However, total number of droplets per unit volume (n/v) is increased with increasing rpm (Re) but the percentage of total water volume can decrease it. For the percentage of water (5, 15%) at 25°C and (5, 10%) at 40°C the number of droplets per unit volume is increased while at 30 % at 25°C and 20% at 40°C the total number of droplets per unit volume drops down due to the fact that they coalesce with each other (Table 3-1,2).

Tables (3-12, 18) for two way analysis shows the effect of rpm (Re) and percentage of water on corrosion rate at (25 °C and 40°C).

At 25 °C both rpm (Re) and percentage of water have significant effect on corrosion rate, but percentage of water is more significant than rpm (Re). At 40°C also rpm (Re) and percentage of water are effective but the percentage of water has more effect than rpm (Re).

The two experiments carried out with different positions of specimens. At 25°C the specimens were placed in the center of the vessel close to rotating shaft and at 40 °C they were placed on the wall of the vessel and it could be the reason to which one effect is more than the other.

By comparing the results, rpm at 25°C is more effective on corrosion than 40°C while percentage of water at 40°C is more effective than 25°C. The reason attributed to the different positions of the specimens, i.e., varying hydrodynamic conditions.

Figures (4-1), (4-2) the calculated corrosion rates are higher than those obtained experimentally. The reason could be attributed to low quantity of water together with rather high temperature (40 °C) which reduces the amount of dissolved oxygen in water. The solubility of oxygen in water decreases significantly with the increase in temperature and slightly with concentration

of dissolved salts⁽⁴⁴⁾. Consequently this would reduce the number of droplets striking the specimen, and very limited area exposed to corrosion. Sometimes this tiny area of corrosion is hardly measured. Moreover the environment of experiments may permit such a difference.

The calculations are normally free from environmental interference, and experience of the researcher. It deals with fixed numbers not liable to any kind of errors.

Figures (4-1)-(4-11) indicate the relation between Re and corrosion rate. This relation is quite normal when Re increases the corrosion rate increased too. Consequently the agitation velocity increased also the droplets formed. Figures (4-8)-(4-21) represent the relation between total number of droplets per unit volume and Re which substantiate.

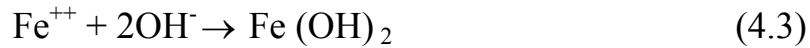
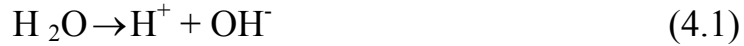
The same explanation is also valid regarding figure (4-22)-(4-28) as related to We, total number of droplets and corrosion rate.

4.3.2 Oxygen concentration

Corrosion can often take place in pipelines or under equipment in which aqueous liquids are being transported (flow differential oxidation corrosion). This usually occurs at positions where there is difference in velocity between different portions of the liquid, i.e. at bends, nozzles, constriction, and etc. when liquid containing oxygen flows rapidly past a given section of pipe the oxygen can be supplied far more quickly to the surface than it can in parts where the liquid is comparatively stagnant. In consequence the stagnant part of the pipe become the anode and corrodes.

The section of the pipe in which water moves rapidly becomes the cathode. This form of corrosion can be avoided only by insuring that the water is properly deoxygenated. Differential oxidation corrosion, of particular importance to the oil industry or other industries where organic liquids are

being stored in steel vessels. If traces of moisture have settled, the bottom of the tank becomes the anode and the following reactions taking place⁽¹⁾:

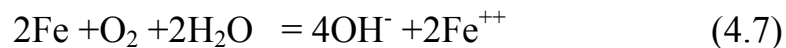


The area of the vessel in contact with the oil or other organic liquids becomes the cathode. Since this area is very large and is kept from corroding by the oil film on top, it acts as a most effective cathode. The oil has oxygen dissolved in it and, in general the amount is sufficiently large to cause a rapid cathode reaction :



As oil often contains NaCl and other salts, reaction is very rapid. The same kind of corrosion is often found in oil pipelines and other equipment containing organic liquids. When the design includes an elbow where water can collect .the rate of corrosion that takes place at the bottom of oil filled vessel is usually rapid because anodic area is small and cathodic area is large⁽⁴⁵⁾.

The following equations explain the mechanism of the reaction between O_2 and Fe to form corrosion where one atom O_2 reacts with two Fe atoms.



Tables (3-5,6,7,8) describe the oxygen transferred. Tables (3-5,6) represent oxygen that causes the corrosion rate by calculating mass transfer coefficient from water phase to the surface of specimen. The oxygen transferred from continuous phase (kerosene) to dispersed phase (water) as a mass transfer coefficient is shown in tables (3-7,8).

Definitely not all the amount of oxygen transferred from continuous phase to dispersed phase (excess) reach the specimen at the same time.

Tables (3-9,10) which represent the corrosion rate calculated on the assumption that all oxygen amount (oxygen soluble in water+ excess) reach the surface of the specimen. So that corrosion rate calculated from the above explanation is greater than the corrosion rate that gained from experimental work.

By comparing tables (3-3,4) for the number of droplets striking the specimen with the total number of droplets formed because of agitation (tables 3-1,2), one can conclude that not all the drops hit the specimen which is in agreement with paragraph mentioned above.

4.3.3 Aqueous Phase

Kerosene contains six times oxygen more than water. In the kerosene /water system, oxygen transfer from kerosene to water and then from water to the metal resulting in corrosion⁽⁴⁶⁾. Water quantity as well as dissolved salts are important in the degree of corrosion. When little amount of water is used, the number of drops are few and consequently less corrosion will taken place. The reason can be attributed to the rather small area in touch between the drops and the specimen surface, resulting in less oxygen transferred to specimen.

Salts dissolved in water have a marked influence on the corrosivity of water. Generally, the corrosivity of water containing dissolved salts increased

with increasing salt. The presence of salts increases the cathodic reaction due to increased of solution electrical conductivity. Since the cathodic reaction should be equal to anodic reaction, therefore, the corrosion will be increased⁽⁴⁷⁾.

4.3.4 Effect of Droplets

The mixing of immiscible liquid phase in among the most important chemical engineering operation ,yet quantitative information on the mixing process is rather lacking .Most available information is applicable only to specialized equipment or to particular liquid system .

In mixing two immiscible fluids energy is transferred to the fluid by the stirrer which serves to suspend the dispersed phase to create turbulence in the fluid.

If the intensity of the turbulence is uniform throughout the tank, the suspended droplets would be subdivided until they reach a size that is no longer affected by the turbulence.

In the usual case the intensity of the turbulence is not uniform through the tank and region of varying intensities exists.

In region of lower intensity, colliding droplets may coalesce, the larger droplets thus formed on passing to regions of higher intensity will again be sheared and broken up. The end state of this sequence of dispersion is a dynamic equilibrium of distribution of droplet size is established throughout the tank.

Droplets are formed during agitation in the kerosene/water system. Kerosene and water do not mix thoroughly, and since the water is less, it changes into droplets distributed in the system. The size and number of droplets depends on the velocity of agitation and water quantity. It is obvious

that the increasing number of droplets will increase the degree of corrosion. The reason could be attributed to rather large amount of oxygen transferred from water to the specimen surface⁽⁴⁸⁾.

When the velocity of agitation is increased, the droplets velocity increased as well. This may result in erosion of specimen by removing of the rust formed and a new surface is exposed to corrosion, thus corrosion increased. Figures below show the relation between number and diameter of droplets and corrosion rate (calculated and experimental) according to tables ((3-5), (3-6) and (3-9), (3-10)) at 25 and 40⁰C . Appendix B shows the relation between droplet diameter (Sauter mean diameter) and Re and corrosion rate (calculated and experimental).

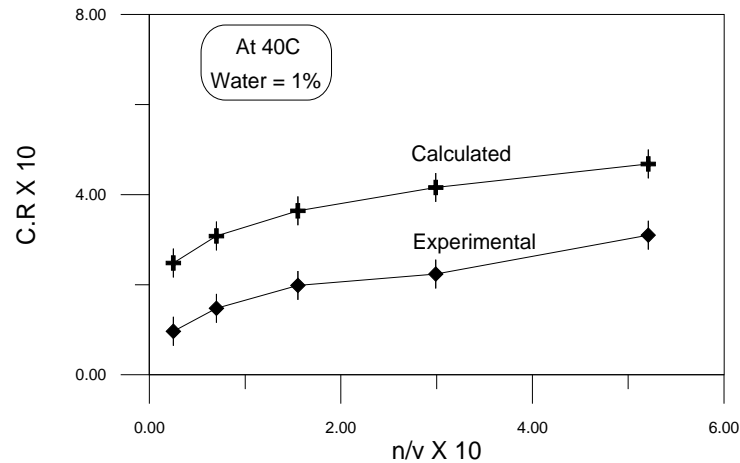


Figure (4-29) Relation between corrosion rate(gmd) (experimental and calculated) vs. number of droplets per unit volume at 40⁰C, %water=0.01.

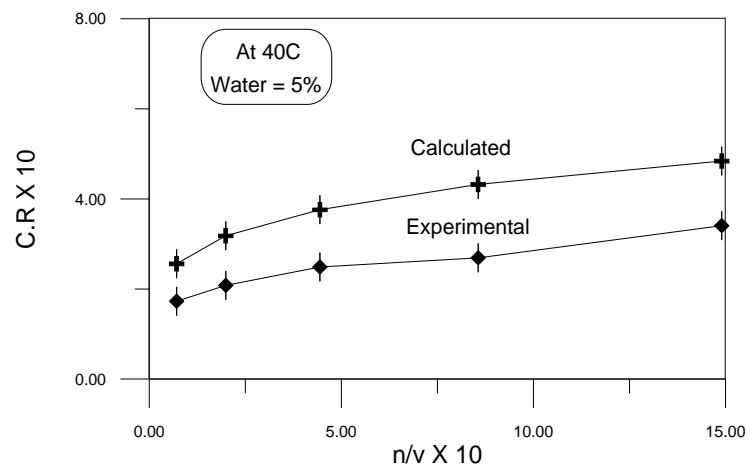


Figure (4-30) Relation between corrosion rate(gmd) (experimental and calculated) vs. number of droplets per unit volume at 40 °C, %water=0.05.

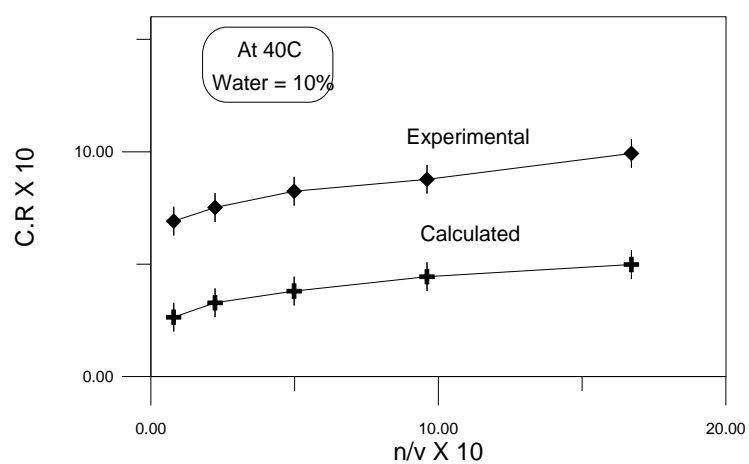


Figure (4-31) Relation between corrosion rate (gmd) (experimental and calculated) vs. number of droplets per unit volume at 40 °C, %water=0.1.

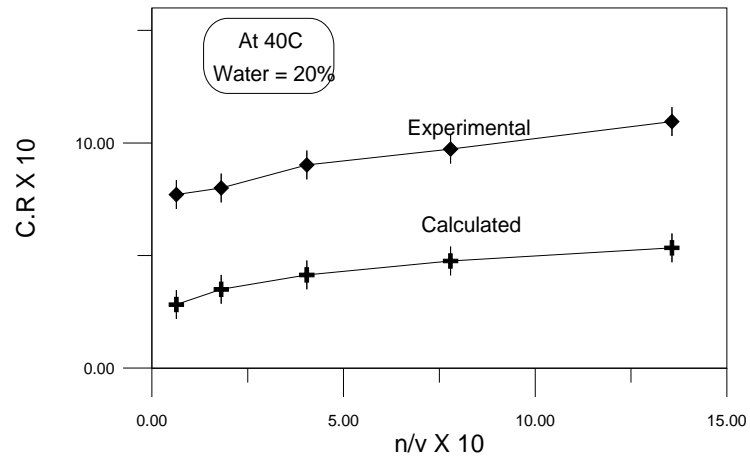


Figure (4-32) Relation between corrosion rate (gmd) (experimental and calculated) vs. number of droplets per unit volume at 40 °C, %water=0.2.

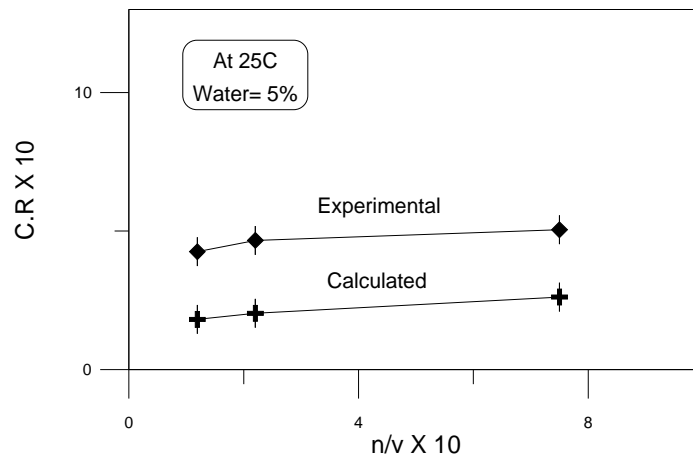


Figure (4-33) Relation between corrosion rate(gmd) (experimental and calculated) vs. number of droplets per unit volume at 25 °C, %water=0.05.

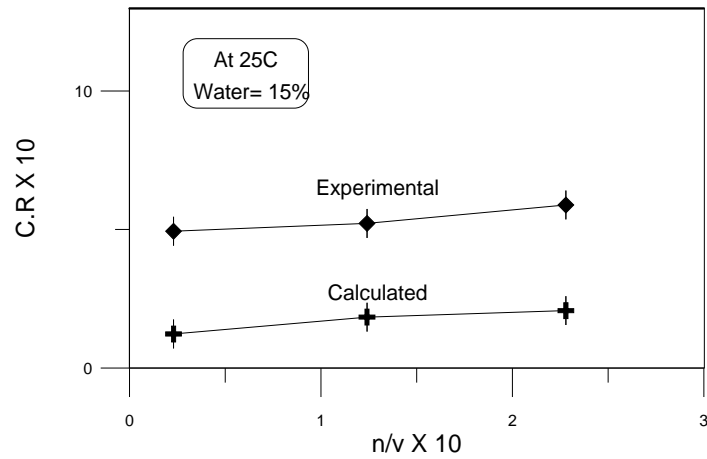


Figure (4-34) Relation between corrosion rate(gmd) (experimental and calculated)vs. number of droplets per unit volume at 25 ⁰C, %water=0.15.

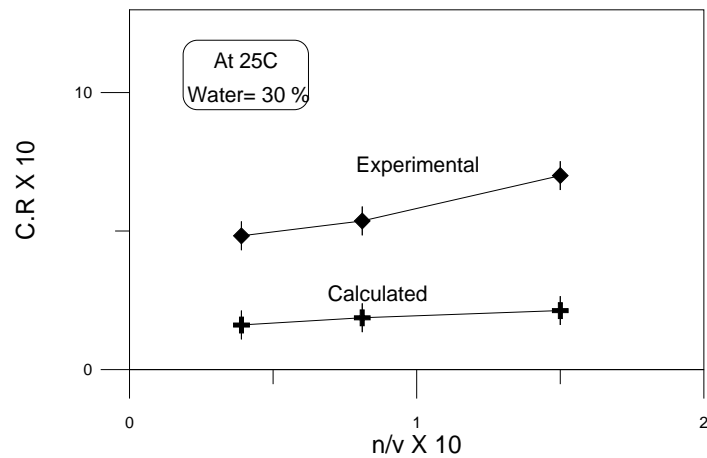


Figure (4-35) Relation between corrosion rate(gmd) (experimental and calculated) vs. number of droplets per unit volume at 25 ⁰C, %water=0.3.

Tables (3-14, 16, 20, 22) for the analysis of the effect of rpm(Re) and percentage of water volume on Sauter mean diameter and number of droplets per unit volume. For Sauter mean diameter (d_{32}) at 25⁰C Table (3-14) shows that both rpm(Re) and percentage of water volume are affective and comparing the results it is found that percentage of water volume is more significant than rpm (Re). At 40⁰C also both rpm and percentage of water volume are affective but the rpm (Re) is more effective than percentage of water volume (Table 3-20).

Table (3-16) shows the effect of rpm (Re) and percentage of water volume on the total number of droplets per unit volume at 25 ⁰C. A corroding to two way analysis it is found that rpm (Re) is significant and percentage ot water volume is not. Table (3-22) for analysis the effect of rpm(Re) and percentage of water volume on the total number of droplets per unit volume at 40⁰C.Re is only effective but percentage of water volume is not regarding total number of droplets per unit volume. Consequently, it can be visualized that corrosion rate under two phase flow agitation is appreciably influenced by both Re(rpm)and percentage of water volume which is more significant, by ANOVA, than Re or rpm at 25 and 40 ⁰C. The Sauter mean diameter dictates the parameter (n/v) which dictates the corrosion rate. The influence of experimental variables (Re or rpm, and percentage of aqueous phase) on Sauter mean diameter depends on the placement of the metal specimens. Both variables affected Sauter mean diameter. At 25 ⁰C Sauter mean diameter is more significantly affected by the percentage of aqueous phase volume when the specimens placed close to impeller shaft. On the other hand, Sauter mean diameter is effected more by Re or rpm when specimens were placed at the vessel wall. Hence corrosion rate under two phase flow, liquid/ liquid, turbulently agitated is markedly influenced by number of droplets per unit volume (n/v) regardless of position in the agitation vessel which is dictated by

impeller Re (rpm) and percentage aqueous volume to an extent dependent on position in the agitation vessel. A summary is shown in the following ANOVA table

Table (4-1) summary of two way analysis at 25 °C.

Level of significans	C.R			n/v			SMD		
0.01	Re	F _{CAL}	F _{TAB}	Re	F _{CAL}	F _{TAB}	Re	F _{CAL}	F _{TAB}
	% aq.	61.39	6.01	% aq.	110.81	18	% aq.	59.38	18
	Vol.	75.73	6.01	Vol.	3.31	18	Vol.	159.38	18
0.05	Re	F _{CAL}	F _{TAB}	Re	F _{CAL}	F _{TAB}	Re	F _{CAL}	F _{TAB}
	% aq.	61.39	3.55	% aq.	110.81	6.94	% aq.	59.38	6.94
	Vol.	75.73	3.55	Vol.	3.31	6.94	Vol.	159.38	6.94

Table (4-2) summary of two way analysis at 40 °C.

Level of significans	C.R			n/v			SMD		
0.01	Re	F _{CAL}	F _{TAB}	Re	F _{CAL}	F _{TAB}	Re	F _{CAL}	F _{TAB}
	% aq.	36.38	5.41	% aq.	44.72	5.41	% aq.	24.52	5.41
	Vol.	675.47	5.95	Vol.	28.55	5.95	Vol.	5.67	5.95
0.05	Re	F _{CAL}	F _{TAB}	Re	F _{CAL}	F _{TAB}	Re	F _{CAL}	F _{TAB}
	% aq.	36.38	3.26	% aq.	44.72	3.26	% aq.	24.52	3.2
	Vol.	675.47	3.49	Vol.	28.55	3.49	Vol.	5.67	3.49

4.3.5 Effect of flow pattern

Agitation is mean whereby mixing phases can be accomplished and by which mass and heat transfer can be enhanced between phases or external surfaces. The operation of agitation, which includes mixing as a special case, is now well established as an important and in a wide variety of chemical processes.

Mixing in tanks is an important area when one considers the number of processes, which are accomplished in tanks, essentially, any physical or transport process can occur during mixing in tanks. Qualitative and quantitative observations, experimental data, and flow regime identifications are needed and should be emphasized in any experimental pilot studies in mixing.

Fluid mechanics and geometry are key points to understand mixing. The fluid mechanics transports the material about the tank, whereas the geometry determines the fluid mechanics. In fact, the geometry is so important that the processes can be considered geometry specific. Liquid-liquid dispersion depend upon the geometry of the impeller; blending, upon the relative size of the tank to the impeller; and power draw, upon the impeller geometry.

Mixing efficiency in a stirred tank is affected by various numbers of parameters such as baffles, impeller speed, impeller type, clearance, tank geometry, solubility of substance, eccentricity of the impeller.

A vortex is produced owing to centrifugal force acting on the rotating liquid. If vortex reaches the impeller severe air entrainment occurs. The depth and the shape of the vortex depend on impeller and vessel dimensions as well as on rotational speed.

Baffles are flat vertical strips set radially along the tank wall, they avoid vortex formation. In baffled tanks, a better concentration distribution throughout the tank occurs and therefore improvement in the mixing efficiency is achieved. The larger the width of the baffles, the better is the mixing to come extend. In the unbaffled vessel with the impeller rotating in the center, centrifugal force acting on the fluid raises the fluid level at the wall and lowers the level at the shaft.

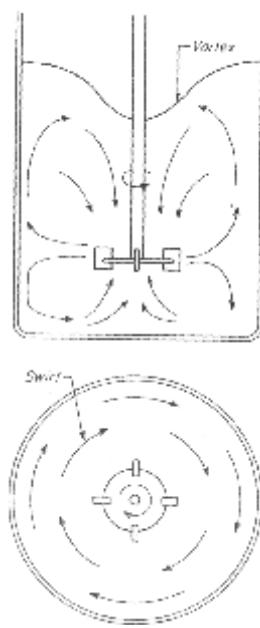


Figure (4-36) Vortex formation and circulation pattern in an agitated tank

Figure (4-36) shows the flow motion in the agitation vessel. Near the impeller (in the center of the vessel) we can recognize a vortex. It effects on the turbulence of the fluid near the impeller which leads for more oxygen to enter the solution (more soluble oxygen) and increase corrosion rate. This is identical with what we conclude from two way analysis Table (3-12, 14).

Near the wall the motion is smooth so the turbulence decreases and Re decreases in comparison with the center of the vessel which leads to decrease the corrosion rate.

CHAPTER FIVE

CONCLUSIONS AND RECOMMENDATIONS

5.1 Conclusions.

The current study revealed some conclusions and facts. These are:

1. Corrosion rate increases with increasing agitation velocity represented by Re. Increasing velocity of agitation causing dispersion of aqueous phase, so the number of droplets increases which leads to increased corrosion rate.
2. A decrease in the diameter of droplets (Sauter mean diameter) attributed to increasing velocity, the more dispersion of the aqueous the less size of droplets and more liability to corrosion.
3. The number of droplets increases with increasing in the total volume of water to certain level then the number of droplets drops down due to coalescence.
4. Local placement of metal specimens in the agitation vessel affects the rate of the corrosion process.

5.2 Recommendations.

The following suggestions could be considered for future work:

1. Using another two phase, e.g. (gas- liquid).
2. Mixing the two phase by bubbling the gas phase from the bottom of the vessel.
3. Using different ranges of agitation velocity.
4. Making the system stable and mix the two phases by rotating the specimen.

References

1. Banerjee S.N.,” an introduction to science of corrosion and its inhibitor”, Oxonian press pvt. LTD., 1985.
2. Walsh F. (1991) Faraday and his law of electrolysis Bulletin of Electrochem 7,11 481-489.
3. Pirre R. Roberge " Hand book of corrosion Eng. ", Mc Grow-Hill ,2000.
4. Ulig H.H., “Corrosion and Corrosion Control”, 3rd Edition., Wiley-Interscience Publicatio, Newyork, 1985.
5. Fontana and Greene,” Corrosion Engineering”, Mc Graw .Hill,1984.
6. Henry S.D. and Scott W.M., Corrosion in the Petrochemical Industry, 1st Edition. ASM International, USA, 1999.
7. Shreir L.L., Jarman R.A.” Corrosion”, 3nd Edition., Newnes-Butter., London, 1994.
8. Stewart D., Tulloch D. S. "Principles of corrosion and protection", Mac millan & co LTD, 1968.
9. Peabody A. W. "Peabody's Control of pipeline corrosion", NACE Inter., 2nd edition, 2001.
10. Nestor Perez, "Electrochemistry of corrosion Science", Kluwer academic publishers, 2004.
11. Talbot D., Talbot J. " Corrosion Science and Technologies", CRC, 1998.
12. Winston R. Revie "Uhlig's corrosion Hand book " 2nd edition, John wiley & Sons, INC. 2000.
13. Thomes J.G.N., The Electrochemistry of corrosion ,Gareth Hinads, 2005.
14. Heitz E. E. and Kreysa G.,” Principles of Electrochemical Eng.”, an Extended Version of a DECHEMA, Experimental Course, VCH, 1986.
15. Harris, A. & A. Marshall "Corrosion prevention and control", 1980.

16. Li C., Tang X., Ayello F., Cai J. and Nesic S., Experimental Study on Water wetting and CO₂ corrosion in oil water two phase flow, ohio university, 2006.
17. Wicks M., Fraser J.P. "Entrainment of water by flowing oil ", Materials Performance, May 1975 p.p 9-12.
18. Smith L.M., Simon M.J.J. and Waard C. de, "Controlling Factors in the Rate of CO₂ Corrosion", UK. Corr.'87 Brighton, 26-28 Oct., 1987.
19. Waard C. de and Lotz U., "Prediction of CO₂ Corrosion of Carbon Steel", Corrosion/93, paper no. 69, (Houston, TX: NACE International, 1993).
20. Adams C. D., Garber J. D., Walters F. H., Singh C., "Verification of Computer Modeled Tubing Life Predictions by Field Data", Corrosion/93, paper no. 82, (Houston, TX: NACE International, 1993).
21. Waard C.de, Smith L. and B.D. Craig, "The Influent of Crude Oil on Well Tubing Corrosion Rates", EUROCORR 2001.
22. Hunsaker, J.C., and B.G. Rightmire, "Eng. Applications of Fluid Mechanics", New York, McGraw-Hill international, 1997, Ch.7.
23. Bakker, A., J.M. Smith and K.J. Myers, "Chem. Eng., 101(12):98(1994).
24. Oldshue, J.Y., "Fluid Mixing Technology, Chemical Eng.", New York, McGraw-Hill international, 1983, P.32.
25. Clift, R.J.R. Grace, and M.E. Weber, "Bubbles, Drops, and Particles", New York Academic Press, 1978.
26. C.J. Genckopie, "Mass transport Phenomena", sixth edition, P.128, 1986.
27. F. A. Holland " Fluid flow for chemical Eng.", 2nd edition, Holland and R. Bragg, 1995.
28. Hu B., L. Lin, Mater O. K., Angeli P., Hewitt G. F., E. S. P. De Ortiz "Investigation of phase inversion of liquid- liquid dispersion in agitation vessels", Vol. 11, 2 April 2006.

29. Wang S., Nesic S., "On coupling CO₂ Corrosion and Multiphase flow model", 2003.
30. Finney D. J., "The Theory of Experimental Design", 3rd edition, 1963.
31. Clark and Schkade, "Statistical method for business decision", South Western, 1969.
32. Siegal S., "nonparametric statistics for the behavioral science", 1995.
33. Trybal, "Mass Transfer Operation", 2004.
34. Brennen C.E., "Cavitation and bubble Dynamics", 1995.
35. Mezaki R., Mochizuki M., Ogama K., "Engineering Data of mixing", Elsevier Science & Technology book, Jan. 2000.
36. Atwaan M., M.Sc. Thesis, Baghdad University, Baghdad, 1986.
37. Aziz H., M.Sc. Thesis, Al- Nahrain University, Baghdad, 2006.
38. Application Statistics of engineering, William Volk, Mc Graw, 2nd edition, 1969.
39. Tretheway K. R. and Chamberlain J., "Corrosion Science and Engineering", 2nd Edition., Longman, London, 1996.
40. "OGJ Special Report," Oil and Gas Journal", August 23, 1999.
41. Fang H., Nesic S., Brown B., "General CO₂ Corrosion in high salinity Brines", Ohio University, 2004.
42. Mizushima T., Matsumoto T., and Yoneda S., , Heat and Mass Transfer Source Book, 1977.
43. Townsend A.A., Fluid Mech., Vol. 11, P. 97, 1961.
44. Sense F., Oxygen Solubility, North California State, 2001.
45. Berger F. B. and Hau K. F., Int. J. heat Mass Trans, Vol.20, P. 1185, 1977.
46. Nelson W.L., "petroleum refinery Eng." fourth edition, 1958.
47. Coulson J. M. and Richardson J. F., Chemical engineering, 5th Edition, Butter Worth Heinemann, Britain, 1998.

48.Koich Asano," Mass Transfer From Fundamental to Modern Industrial Applications", Wiley – VCH Verlag GmbH & Co. KGaA , 2006.

Appendix A

Mohammed 's Thesis parameters (25 °C):

Total volume of the mixture (water + kerosene)= 3600 ml

Specimen parameter:

❖ Carbon steel, 12mm diameter, 300 mm length.

Water percent used:

❖ 5%, 15%, 30%.

Agitation tank and turbine parameter:

❖ $L = 22.4$ mm.

❖ $W = 17.9$ mm.

❖ $D_a = 9$ cm.

❖ $H = D_t$.

❖ $J = D_t / 10$.

❖ $D_t = 16.6$ cm.

❖ 6- Blade disc impeller.

Physical properties of water of kerosene at 25 °C.

❖ $\rho_{\text{water}} = 997.06 \text{ Kg/m}^3$, $\rho_{\text{kerosen.}} = 777.722 \text{ Kg/m}^3$ ⁽⁴⁸⁾.

❖ $\mu_{\text{water}} = 0.8937 \text{ cp}$, $\mu_{\text{kerosen}} = 2.5 \text{ cp}$ ⁽⁴⁸⁾.

❖ Solubility = 8.25 mg/lit⁽⁴⁴⁾.

Hussein 's Thesis parameters (40 °C):

Total volume of the mixture (water + kerosene)= 12.2 ml

Specimen parameter:

❖ Carbon steel, 5mm diameter, 2.5 mm length.

Water percent used:

❖ 1%, 5%, 10%, 20%.

Agitation tank and turbine parameter:

❖ $L = 2\text{cm}$.

❖ $W = 1.6\text{ cm}$.

❖ $D_a = 8\text{cm}$.

❖ $H = 30\text{ cm}$.

❖ $J = 2\text{ cm}$.

❖ $D_t = 24\text{ cm}$.

❖ 6- Blade disc impeller.

Physical properties of water of kerosene at 40 °C.

❖ $\rho_{\text{water.}} = 992.25\text{ Kg/m}^3$, $\rho_{\text{kerosen.}} = 773.955\text{ Kg/m}^3$ ⁽⁴⁸⁾.

❖ $\mu_{\text{water}} = 0.656\text{ cp}$, $\mu_{\text{kerosen}} = 2.1\text{cp}$ ⁽⁴⁸⁾.

❖ Solubility = 6.4 mg/lit⁽⁴⁴⁾.

Appendix B

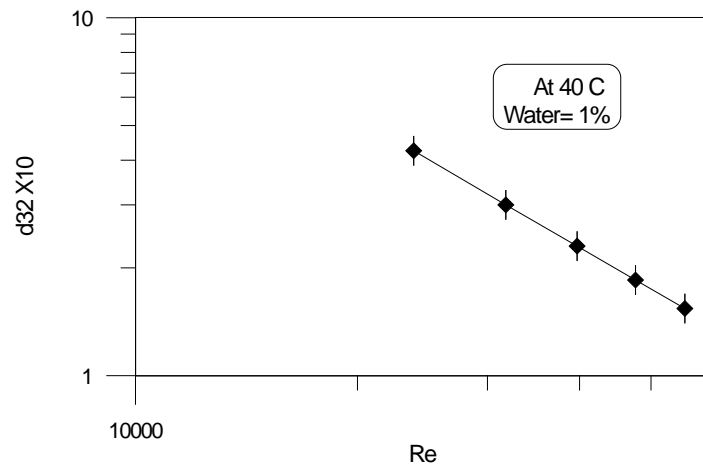


Fig (B-1) Relation between log Sauter mean diameter and log Re at 40 °C
,% water=0.01.

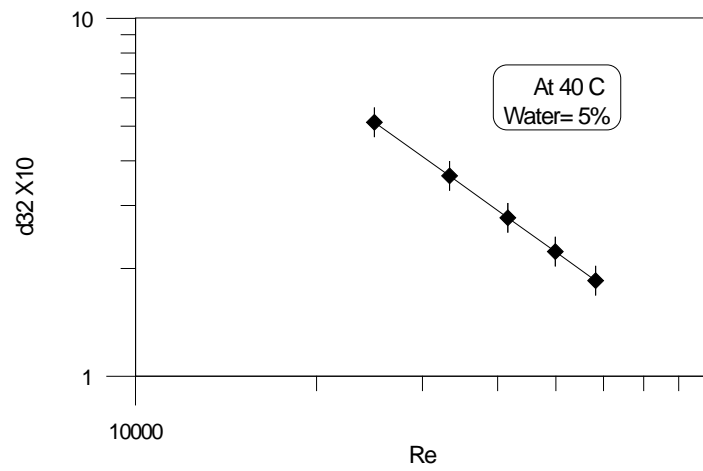


Fig (B-2) Relation between log Sauter mean diameter and log Re at 40°C
,% water=0.05.

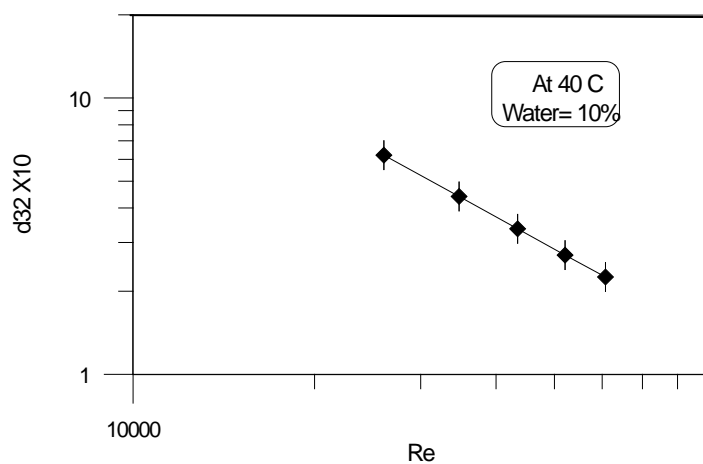


Fig (B-3) Relation between log Sauter mean diameter and log Re at 40⁰C
, % water=0.1.

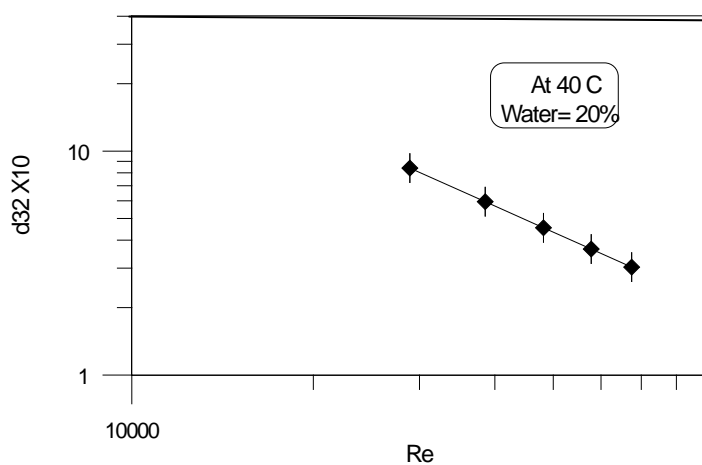
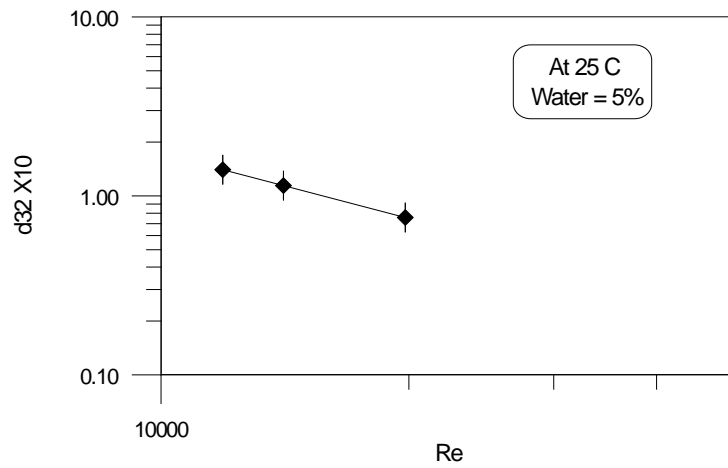


Fig (B-4) Relation between log Sauter mean diameter and log Re at 40⁰C
, % water=0.2.



Fig(B-5) Relation between log Sauter mean diameter and log Re at 25⁰C
,% water=0.5.

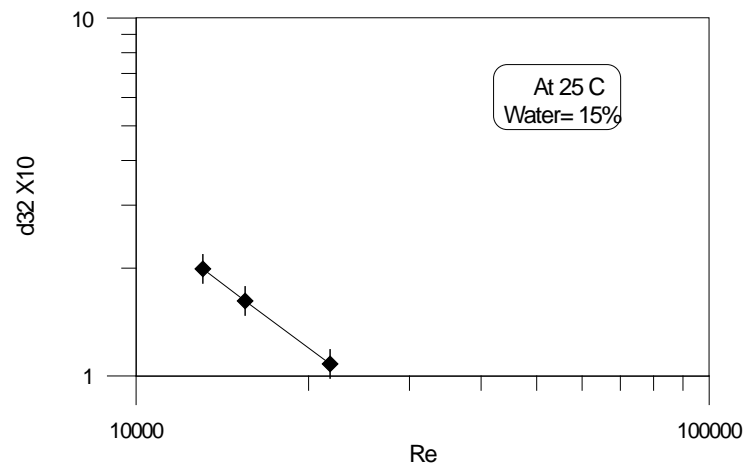


Fig (B-6) Relation between log Sauter mean diameter and log Re at 25⁰C
,% water=0.15.

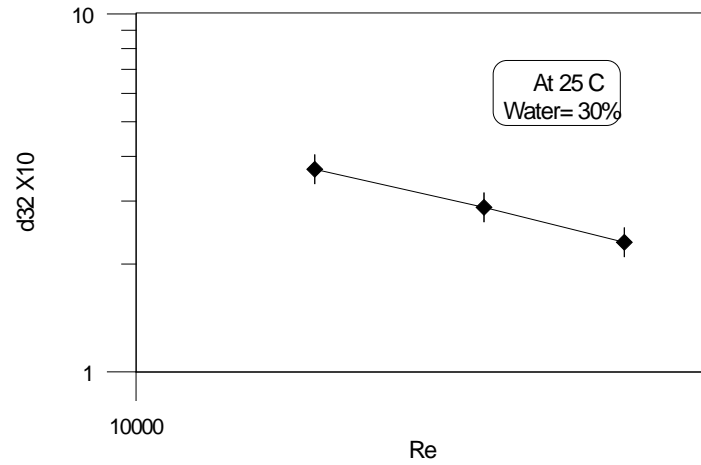


Fig (B-7) Relation between log Sauter mean diameter and log Re at 25⁰C
, % water=0.3.

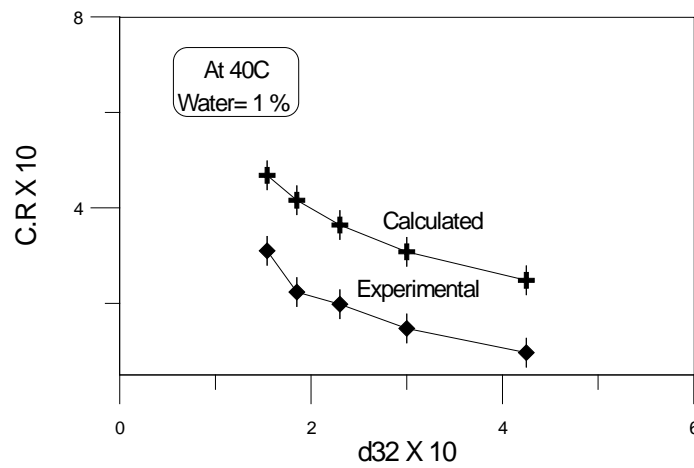


Fig (B-8) Relation between corrosion rate (experimental and calculated) vs.
Sauter mean diameter of droplets at 40⁰C, % water=0.01.

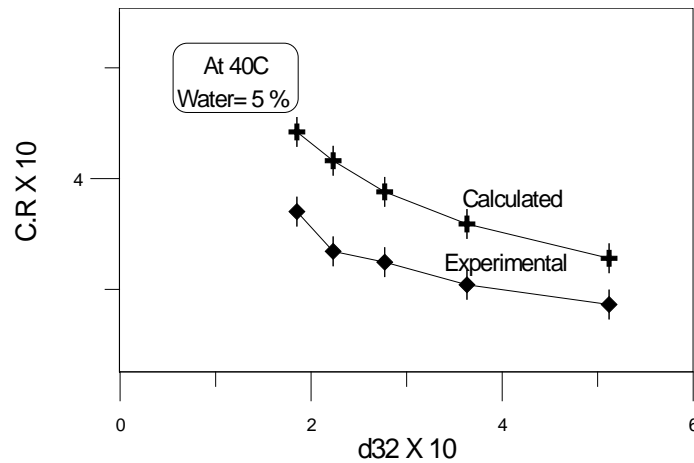


Fig (B-9) Relation between corrosion rate (experimental and calculated) vs. Sauter mean diameter of droplets at 40 °C, % water=0.05.

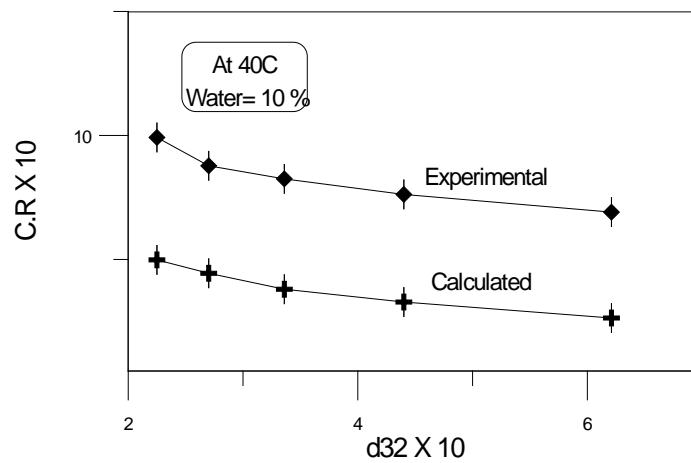


Fig (B-10) Relation between corrosion rate (experimental and calculated) vs. Sauter mean diameter of droplets at 40 °C, % water=0.1.

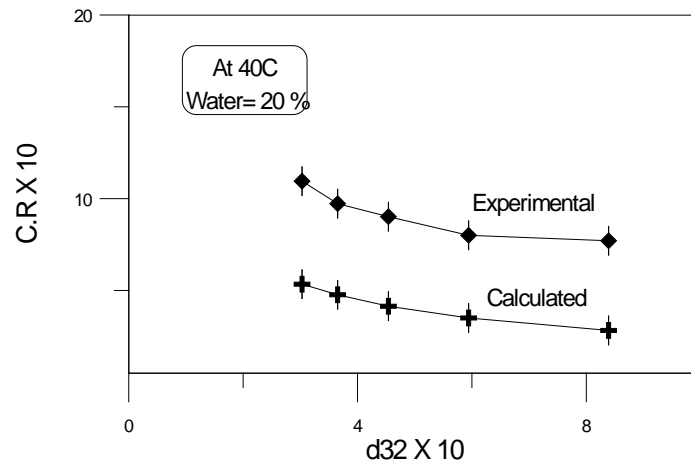


Fig (B-11) Relation between corrosion rate (experimental and calculated) vs. Sauter mean diameter of droplets at 40 °C, %water=0.2.

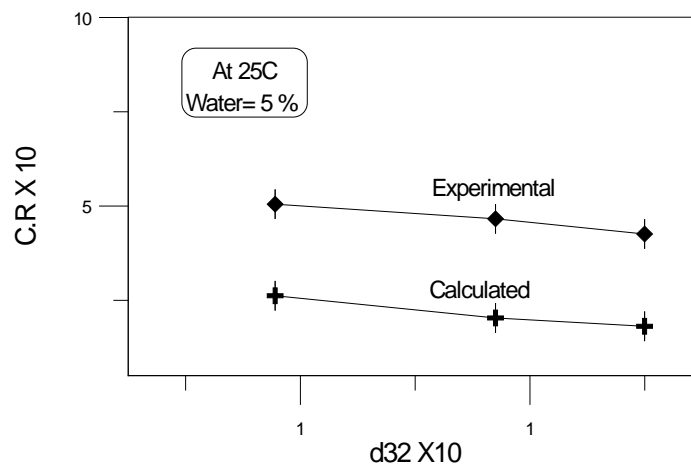


Fig (B-12) Relation between corrosion rate (experimental and calculated) vs. Sauter mean diameter of droplets at 25 °C, %water=0.05.

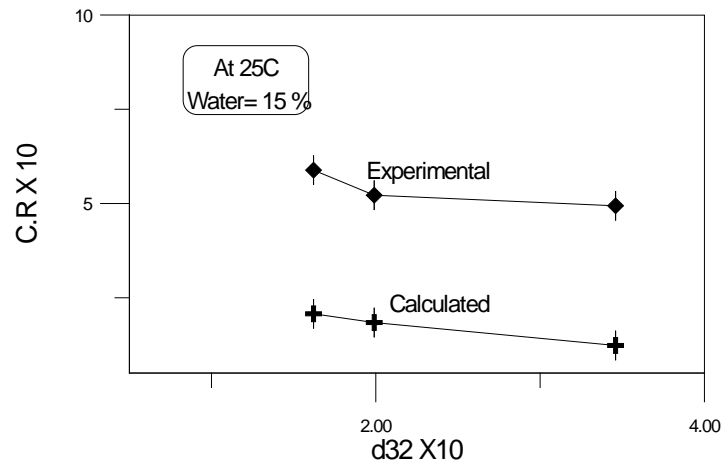


Fig (B-13) Relation between corrosion rate (experimental and calculated) vs. Sauter mean diameter of droplets at 25 °C, % water=0.15.

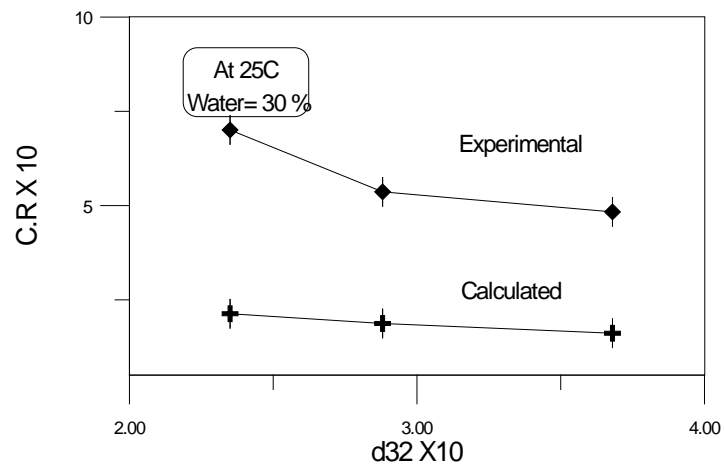
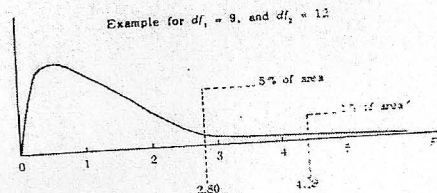


Fig (B-14) Relation between corrosion rate (experimental and calculated) vs. Sauter mean diameter of droplets at 25 °C, % water=0.3.

Appendix C

F DISTRIBUTION



PERCENTAGE POINTS OF THE F DISTRIBUTION*									
df_2	P	$df_1 = 1$	2	3	4	5	6	7	8
1	0.500	1.00	1.50	1.71	1.82	1.89	1.94	1.98	2.00
	0.100	39.9	49.5	53.6	55.8	57.2	58.2	58.9	59.4
	0.050	161	200	216	225	230	234	237	239
	0.025	648	800	864	900	922	937	948	957
	0.010	4,050	5,000	5,400	5,620	5,760	5,860	5,930	5,980
	0.005	16,200	20,000	21,600	22,500	23,100	23,400	23,700	23,900
2	0.001	405,284	500,000	540,379	562,500	576,405	585,937	591,144	598,144
	0.500	0.667	1.00	1.13	1.21	1.25	1.28	1.30	1.32
	0.100	8.53	9.00	9.16	9.24	9.29	9.33	9.35	9.37
	0.050	18.5	19.0	19.2	19.2	19.3	19.3	19.4	19.4
	0.025	38.5	39.0	39.2	39.2	39.3	39.3	39.4	39.4
	0.010	98.5	99.0	99.2	99.2	99.3	99.3	99.4	99.4
3	0.005	199	199	199	199	199	199	199	199
	0.001	998.5	999.0	999.2	999.2	999.3	999.3	999.3	999.4
	0.500	0.585	0.881	1.00	1.06	1.10	1.13	1.15	1.16
	0.100	5.54	5.46	5.39	5.34	5.31	5.28	5.27	5.25
	0.050	10.1	9.55	9.28	9.12	9.01	8.94	8.89	8.85
	0.025	17.4	16.0	15.4	15.1	14.9	14.7	14.6	14.5
4	0.010	34.1	30.8	29.5	28.7	28.2	27.7	27.7	27.5
	0.005	55.6	49.8	47.5	46.2	45.4	44.3	44.4	44.1
	0.001	167.5	148.5	141.1	137.1	134.6	132.3	130.6	130.6
	0.500	0.549	0.828	0.941	1.00	1.04	1.06	1.08	1.09
	0.100	4.54	4.32	4.19	4.11	4.05	4.01	3.98	3.95
	0.050	7.71	6.94	6.59	6.39	6.26	6.15	6.09	6.04
5	0.025	12.2	10.6	9.98	9.60	9.36	9.23	9.07	8.98
	0.010	21.2	18.0	16.7	16.0	15.5	15.2	15.0	14.8
	0.005	31.3	26.3	24.3	23.2	22.5	22.1	21.6	21.4
	0.001	74.1	61.3	56.2	53.4	51.7	50.5	49.0	49.0
	0.500	0.528	0.799	0.907	0.965	1.00	1.02	1.04	1.05
	0.100	4.06	3.78	3.62	3.52	3.45	3.40	3.37	3.34
6	0.050	6.61	5.79	5.41	5.19	5.05	4.95	4.88	4.82
	0.025	10.0	8.43	7.76	7.39	7.15	6.98	6.85	6.76
	0.010	16.3	13.3	12.1	11.4	11.0	10.7	10.5	10.3
	0.005	22.8	18.3	16.5	15.6	14.9	14.5	14.2	14.0
	0.001	47.0	36.6	33.2	31.1	29.3	28.3	27.6	27.6
	0.500	0.515	0.780	0.886	0.942	0.977	1.00	1.02	1.03
7	0.100	3.73	3.46	3.29	3.18	3.11	3.05	3.01	2.98
	0.050	5.99	5.14	4.76	4.53	4.39	4.28	4.21	4.15
	0.025	8.81	7.26	6.60	6.23	5.99	5.82	5.70	5.60
	0.010	13.7	10.9	9.78	9.15	8.75	8.47	8.26	8.10
	0.005	18.6	14.5	12.9	12.0	11.5	11.1	10.8	10.6
	0.001	35.5	27.0	23.7	21.9	20.8	20.0	19.3	19.0

الخلاصة

تكملة لتجارب عزيز و عطوان التحليل النظري استخدم لمعرفة تأثير وجود طورين على التآكل في درجتين حراريتين مختلفتين هما 25 و 40م. وايضا لفهم تأثير خلط هذين الطورين بسرعه مختلفة .

استعمل سائلين رئيسيين في هذه الدراسة هما الماء و الكيروسين. كان الماء المستخدم بنسب مئوية مختلفة من مجموع الحجم الكلي. وهذه النسب المئوية تتراوح من 1% الى 30%. لقد درس تأثير سرعة الخلط و النسب المئوية للماء على التآكل وسجلت النتائج.

ولتقيم النتائج استخدمت طريقة التحليل الاحصائي. اوضحت هذه الطريقة بأنه في درجة حرارة 25م⁰ ان سرعة الخلط لها تأثير واضح على التآكل , عدد القطيرات في وحدة الحجم وعلى قطر هذه القطيرات.

لقد وجد ان النسبة المئوية للماء تؤثر على معدل التآكل وعلى قطر القطيرات المتكونة , ومن جانب اخر فقد لوحظ بان النسبة المئوية للماء ليس لها اي تأثير على عدد القطيرات المتكونة في وحدة الحجم. على اية حال فقد وجد ان تأثير النسبة المئوية للماء على معدل التآكل هي اكثر من تأثير سرعة الخلط. وهذه ايضا حقيقة تنطبق على قطر القطيرات المتكونة .

اظهرت دراسة التحليل الاحصائي في درجة 40م⁰ بأن سرعة الخلط تؤثر على معدل التآكل, عدد القطيرات في وحدة الحجم و قطر القطيرات المتكونة. اضافة الى ذلك فإن التحليل الاحصائي اثبت بان النسبة المئوية للماء لها تأثير اكثر على معدل التآكل في حين ان سرعة الخلط لها تأثير اكبر على قطر القطيرات المتكونة.

ان هذه النتائج تطابقت كذلك من نتائج التجارب التي طبقت في هذه التحاليل. كما وجد ايضا انه كلما ارتفعت درجة الحرارة قل التآكل الحاصل وهذا يعزى الى حقيقة ان ارتفاع درجة الحرارة يقلل الاوكسجين في الطور المائي ولذلك يقل معدل التآكل.

كما أظهر التحليل الاحصائي ان مكان وضع النموذج في أناء الخلط له تأثير ايضا. حيث ان النماذج التي تكون قريبة من محور الدوران تتأثر بشكل مختلف عن النماذج الموضوعة على جدران اناء الخلط. وهذا يعزى الى شدة الاضطراب وعدد القطيرات في وحدة الحجم وذلك بسبب كون شدة الاضطراب وعدد القطيرات في وحدة الحجم ليست متشابهة ومتساوية في المواقع المختلفة في اناء الخلط

شكر وتقدير

اشكر الله عز وجل الذي وفقني لاكمال متطلبات هذا البحث. وانا انهي بحثي لا يسعني واعترافا بالفضل الا ان اتقدم بوافر الشكر والامتنان للاستاذ المشرف الدكتور قاسم جبار سليمان لاشرافه ولمواصلته ومتابعته العلمية للبحث وما ترتب على ذلك من توجيهات قيمه واءراء سديدة.

واتقدم بجزيل الشكر الى جميع اساتذة قسم الهندسة الكيمياوية لمساعدتهم القيمة لي طيلة فترة الدراسة ولمدهم يد العون لي خلال اعداد هذه الرسالة.

ولا استطيع ان انسى فضل والدي العزيزين واخي لمساعدتي لانجاز هذا البحث ومساندتهم لي لتخطي الصعوبات التي واجهتني.

وشكري الجزيل الى جميع زملائي و زميلاتي الذين ساعدوني عند حاجتي اليهم.

مريم حسين فوزي

التحليل النظري لتآكل الكربون ستيل في حالة وجود طورين

رسالة

مقدمة إلى كلية الهندسة في جامعة نهرين
وهي جزء من متطلبات نيل درجة ماجستير علوم
في الهندسة الكيمياوية

من قبل

مريم حسين فوزي

(بكالوريوس علوم في الهندسة الكيمياوية 2005)

1430

2009

محرم

كانون الثاني